arXiv:math-ph/0407075 v3 22 Jul 2005

Continuous Limit of Discrete Sawtooth Maps and its Algebraic Framework

FABIO BENATTI
Dipartimento di Fisica Teorica
Università di Trieste
and Istituto Nazionale di Fisica Nucleare, Sezione di Trieste,
Strada Costiera 11, 34014 Trieste, Italy
fabio.benatti@ts.infn.it

VALERIO CAPPELLINI
Dipartimento di Fisica Teorica
Università di Trieste
Strada Costiera 11, 34014 Trieste, Italy
valerio.cappellini@ts.infn.it

23rd January 2006

Abstract

We study the presence of a logarithmic time scale in discrete approximations of Sawtooth Maps on the 2–torus. The techniques used are suggested by quantum mechanical similarities, and are based on a particular class of states on the torus, that fulfill dynamical localization properties typical of quantum Coherent States.

Keywords: Chaos; discrete systems; automorphisms on the 2–torus; semi–classical limit; coherent states.

Mathematics Subject Classification 2000: 37D20; 81Q20, 81R30, 46L99

Contents

1. Introduction

Under the term of Quantum Chaos goes a rich phenomenology of behaviours [1–3] proper to quantum systems whose classical limit presents typical chaotic features as positive Lyapunov exponents (hyperbolic regime) [4–6].

The footprints of classical chaos are usually studied semi–classically when a suitable "$\hbar$"–like quantization parameter goes to zero; one then examines the differences between quantum and classical behaviours. In the hyperbolic case, quantum chaos reveals itself through the presence of a time–scale, over which quantum and classical motions mimic each other, that increases as $-\log$"$\hbar$" [1–3,7–9]. This peculiar logarithmic time scale has to be compared with the scaling "$\hbar$"$^{-\alpha}$, $\alpha > 0$, which is proper of quantum systems with regular classical limit [1].

Heuristical explanations of the logarithmic time-scale already indicate that the phenomenon is not exclusive of quantum systems, and thus of non–commutativity, but that it should also be present when the classical dynamics is looked at as the continuous limit of a family of discrete classical systems. [10].

Intrinsically discrete systems [11] and discretized classical continuous systems [12–14] have recently been objects of numerical analysis concerning the entropy production and the presence of a logarithmic time scale, whereas the ergodic properties of discretized discontinuous maps have been addressed in [15].

In the following, we shall rigorously show this fact to be true for Sawtooth Maps on the 2-dimensional torus [16–18]: this will be done by forcing them to move on a square lattice and by retrieving the continuous dynamics when the lattice spacing goes to zero. Because of the analogies between quantization and discretization, we will make use of technologies strictly resembling the so-called *Anti–Wick* quantization [19].

We shall prove that a time–scale logarithmic in the lattice-spacing appears; in comparison to previous results obtained studying numerically the entropy production [14], a rigorous continuous limit is established that succeeds in controlling the discontinuities of Sawtooth Maps. Despite their classical nature, the entropy previously investigated was quantum mechanical; somewhat analogously, in this article, Sawtooth Maps will be studied by means of states, which play a role similar to quantum Coherent States, whose choice is naturally provided by the lattice structure of discretized Sawtooth Maps. They will be shown to satisfy a *dynamical localization property* that makes them remain localized around the trajectories of the continuous dynamics, but only on a logarithmic time scale.

2. Classical Dynamical Systems

Classical dynamics is usually described by means of a measure space $\mathcal{X}$, the phase–space, endowed with the Borel σ–algebra and a normalized measure μ, $\mu(\mathcal{X}) = 1$. The "volumes"

$$\mu(E) = \int_E \mu(\mathrm{d}\boldsymbol{x})$$

of measurable subsets $E \subseteq \mathcal{X}$ represent the probabilities that a phase–point $\boldsymbol{x} \in \mathcal{X}$ belong to them: the measure μ defines the statistical properties of the system and represents a possible state, which is taken to be an equilibrium state with respect to the given dynamics.

In such a scheme, a reversible discrete time dynamics amounts to an invertible measurable map $S : \mathcal{X} \mapsto \mathcal{X}$ such that $\mu \circ S = \mu$ and to its iterates $\{S^k \mid k \in \mathbb{Z}\}$: phase–trajectories passing through $\boldsymbol{x} \in \mathcal{X}$ at time 0 are then sequences $\left\{S^k \,\boldsymbol{x}\right\}_{k\in\mathbb{Z}}$ [6].

Classical dynamical systems are thus conveniently described by triplets $(\mathcal{X}, \mu, S)$; in the present work, we shall focus upon the following choices:

$\mathcal{X}$: the 2–dimensional torus $\mathbb{T}^2 = \mathbb{R}^2/\mathbb{Z}^2 = \left\{\boldsymbol{x} = (x_1, x_2) \in \mathbb{R}^2 \pmod 1\right\}$;

μ: the Lebesgue measure, $\mu(\mathrm{d}\boldsymbol{x}) = \mathrm{d}x_1\,\mathrm{d}x_2$, on $\mathbb{T}^2$;

S: an invertible measurable transformations on $\mathbb{T}^2$ that preserves the Lebesgue measure.

It is convenient to associate an algebraic triple $(\mathcal{M}, \omega, \Theta)$ to the measure–theoretic triple $(\mathbb{T}^2, \mu, S)$, consisting of

$\mathcal{M}$: the (Abelian) Von Neumann *-algebra $L^\infty_\mu\left(\mathbb{T}^2\right)$ of essentially bounded functions on $\mathbb{T}^2$ [20, 21].

ω_μ: the state (expectation) on $\mathcal{M}$, given by

$$\omega_\mu : L^\infty_\mu\left(\mathbb{T}^2\right) \ni f \longmapsto \omega_\mu(f) := \int_{\mathbb{T}^2} \mu(\mathrm{d}\boldsymbol{x})\ f(x) \in \mathbb{R}^+ \cdot \tag{1}$$

Θ: the automorphism of $\mathcal{M}$ such that $\Theta(f) = f \circ S$, $\omega \circ \Theta = \omega$.

In the following, we shall consider a discretized version of $(\mathbb{T}^2, \mu, S)$ which arises by forcing the continuous classical system to live on a square lattice $L_N \subseteq \mathbb{T}^2$ of spacing $\frac{1}{N}$:

$$L_N := \left\{ \frac{\boldsymbol{p}}{N} \;\middle|\; \boldsymbol{p} \in (\mathbb{Z}/N\mathbb{Z})^2 \right\} \ , \tag{2}$$

where $(\mathbb{Z}/N\mathbb{Z})$ denotes the residual class $(\mathrm{mod}\ N)$, that is $0 \leqslant p_i \leqslant N-1$.

Taking the N^2 points as labels of the elements $\{|\boldsymbol{\ell}\rangle\}_{\boldsymbol{\ell}\in(\mathbb{Z}/N\mathbb{Z})^2}$ of an orthonormal basis (o.n.b.) of the $\mathcal{N}$ dimensional Hilbert space $\mathcal{H}_\mathcal{N}$, $\mathcal{N} := N^2$, we will consider discrete algebraic triples $\left(\mathcal{D}_\mathcal{N}, \tau_\mathcal{N}, \Theta_\mathcal{N}\right)$, consisting of

$\mathcal{D}_\mathcal{N}$: an $\mathcal{N} \times \mathcal{N}$ matrix algebra diagonal in the orthonormal basis introduced above;

$\tau_\mathcal{N}$: the uniform state (expectation) on $\mathcal{D}_\mathcal{N}$ defined by

$$\tau_\mathcal{N} : \mathcal{D}_\mathcal{N} \ni D \longmapsto \tau_\mathcal{N}(D) := \frac{1}{\mathcal{N}}\,\mathrm{Tr}\,(D) \in \mathbb{R}^+ \ ; \tag{3}$$

$\Theta_\mathcal{N}$: an automorphism of $\mathcal{D}_\mathcal{N}$ suitably reproducing Θ when $N \longrightarrow \infty$ (see Section 4.2).

Remark 2.1

As it will become evident in the following, up to a certain extent, discretization resembles quantization; in the latter case, instead of $\mathcal{D}_\mathcal{N}$, one deals with non–commutative matrix algebras, the typical instance being the finite dimensional quantization of the Arnold Cat Map [22, 23].

3. Discretization of phase–space

As sketched in the previous Remark, we proceed now to setup a discretization procedure close to the so–called Anti–Wick quantization [19].

Given the classical algebraic triple $\left(L^\infty_\mu\left(\mathbb{T}^2\right), \omega_\mu, \Theta\right)$, the aim of a discretization–dediscretization procedure (specifically an $\mathcal{N}$–dimensional discretization) is twofold:

- finding a pair of *-morphisms, $\mathcal{J}_{\mathcal{N},\infty}$ mapping $L^\infty_\mu\left(\mathbb{T}^2\right)$ into the abelian finite dimensional algebra $\mathcal{D}_\mathcal{N}$ and $\mathcal{J}_{\infty,\mathcal{N}}$ mapping backward $\mathcal{D}_\mathcal{N}$ into $L^\infty_\mu\left(\mathbb{T}^2\right)$;
- providing an automorphism $\Theta_\mathcal{N}$, the discrete dynamics, acting on $\mathcal{D}_\mathcal{N}$ such that it approximates the continuous one, Θ, on $L^\infty_\mu\left(\mathbb{T}^2\right)$ as follows

$$\mathcal{J}_{\infty,\mathcal{N}} \circ \Theta^j_\mathcal{N} \circ \mathcal{J}_{\mathcal{N},\infty} \xrightarrow[N\to\infty]{} \Theta^j \quad . \tag{4}$$

The latter requirement can be seen as a modification of the so called Egorov's property (see [24]). Intuitively, a discrete description of the measure–theoretic triple $\left(\mathbb{T}^2, \mu, S\right)$ becomes finer when we increase N, the number of points per linear dimension on the grid L_N in (2): this corresponds to enlarging the dimension of the Hilbert space $\mathcal{H}_\mathcal{N}$ associate to the corresponding algebraic triple $\left(\mathcal{D}_\mathcal{N}, \tau_\mathcal{N}, \Theta_\mathcal{N}\right)$. In this sense, the lattice spacing $a := \frac{1}{N}$ of the grid L_N is a natural "discretization parameter" playing an analogous role to the quantization parameter $\hbar$.

The difficulty is to find convenient *-morphisms $\mathcal{J}_{\mathcal{N},\infty}$ and $\mathcal{J}_{\infty,\mathcal{N}}$ that set up a rigorous asymptotic (in N) correspondence, of functions on $L^\infty_\mu\left(\mathbb{T}^2\right)$ and matrices in $\mathcal{D}_\mathcal{N}$ and, above all, between the discrete dynamics $\Theta_\mathcal{N}$ and the continuous one Θ.

Due to the similarities with quantization, we shall consider a discretization procedure based on states that we shall refer to as Lattice States (LS for short) which mimic the use of Coherent States in the study of the semi–classical limit. In the next section we will give a suitable definitions of LS belonging to the Hilbert space $\mathcal{H}_\mathcal{N}$, that we shall use to discretize $\left(L^\infty_\mu\left(\mathbb{T}^2\right), \omega_\mu, \Theta\right)$.

3.1. Lattice States on $\mathbb{T}^2$

In analogy with the the properties of quantum Coherent States, we shall look for a class $\{|C_\mathcal{N}(\boldsymbol{x})\rangle \mid \boldsymbol{x} \in \mathbb{T}^2\} \in \mathcal{H}_\mathcal{N}$ of vectors, indexed by points $\boldsymbol{x} \in \mathbb{T}^2$, satisfying the following conditions which are borrowed from analogous quantum ones [25]:

Properties 3.1

1. Measurability: $\boldsymbol{x} \mapsto |C_{\mathcal{N}}(\boldsymbol{x})\rangle$ is measurable on $\mathbb{T}^2$;

2. Normalization: $\|C_{\mathcal{N}}(\boldsymbol{x})\|^2 = 1$, $\boldsymbol{x} \in \mathbb{T}^2$;

3. Completeness: $\mathcal{N} \int_{\mathbb{T}^2} \mu(\mathrm{d}\boldsymbol{x})\, |C_{\mathcal{N}}(\boldsymbol{x})\rangle\langle C_{\mathcal{N}}(\boldsymbol{x})| = \mathbb{1}$;

4. Localization: given $\varepsilon > 0$ and $d_0 > 0$, there exists $N_0(\epsilon, d_0)$ such that for $N \geq N_0(\epsilon, d_0)$ and $d_{\mathbb{T}^2}(\boldsymbol{x}, \boldsymbol{y}) \geq d_0$ one has
$$\mathcal{N}\, |\langle C_{\mathcal{N}}(\boldsymbol{x}), C_{\mathcal{N}}(\boldsymbol{y})\rangle|^2 \leq \varepsilon .$$

The symbol $d_{\mathbb{T}^2}(\boldsymbol{x}, \boldsymbol{y})$ used in the localization property stands for the length of the shorter segment connecting the two points $\boldsymbol{x}, \boldsymbol{y} \in \mathbb{T}^2$, namely

Definition 3.1

We shall denote by $d_{\mathbb{T}^2}(\boldsymbol{x}, \boldsymbol{y}) := \min_{\boldsymbol{n} \in \mathbb{Z}^2} \|\boldsymbol{x} - \boldsymbol{y} + \boldsymbol{n}\|_{\mathbb{R}^2}$ the distance on $\mathbb{T}^2$.

We shall now construct a family of $|C_{\mathcal{N}}(\boldsymbol{x})\rangle$. Let $\lfloor \cdot \rfloor$ denote the integer part of a real number, namely $x - 1 < \lfloor x \rfloor \leqslant x$ is the largest integer smaller than x; further, let $\langle \cdot \rangle$ denote the fractional parts, that is $\langle x \rangle := x - \lfloor x \rfloor$. Thus we will write

$$\mathbb{T}^2 \ni \boldsymbol{x} = \left(\frac{\lfloor N x_1 \rfloor}{N}, \frac{\lfloor N x_2 \rfloor}{N} \right) + \left(\frac{\langle N x_1 \rangle}{N}, \frac{\langle N x_2 \rangle}{N} \right) ,$$

or, more compactly, $\boldsymbol{x} = \dfrac{\lfloor N\boldsymbol{x} \rfloor}{N} + \dfrac{\langle N\boldsymbol{x} \rangle}{N}$. We proceed by associating to points of $\mathbb{T}^2$ specific lattice points.

Definition 3.2 (Lattice States)

Given $\boldsymbol{x} \in \mathbb{T}^2$, we shall denote by $\hat{\boldsymbol{x}}_N$ the element of $(\mathbb{Z}/N\mathbb{Z})^2$ given by

$$\hat{\boldsymbol{x}}_N = (\hat{x}_{N,1}, \hat{x}_{N,2}) := \left(\lfloor N x_1 + \tfrac{1}{2} \rfloor \,,\, \lfloor N x_2 + \tfrac{1}{2} \rfloor \right) , \tag{5}$$

and call Lattice States on $\mathbb{T}^2$ the vectors $|C_{\mathcal{N}}(\boldsymbol{x})\rangle$ defined by

$$\mathbb{T}^2 \ni \boldsymbol{x} \mapsto |C_{\mathcal{N}}(\boldsymbol{x})\rangle := |\, \hat{\boldsymbol{x}}_N \rangle \in \mathcal{H}_{\mathcal{N}} \,\cdot \tag{6}$$

Remark 3.1

The family of states $|C_{\mathcal{N}}(\boldsymbol{x})\rangle$ is constructed by choosing, for each $\boldsymbol{x} \in \mathbb{T}^2$, that element of the basis of $\mathcal{H}_{\mathcal{N}}$ which is labeled by the closest element of L_N to $\boldsymbol{x}$.

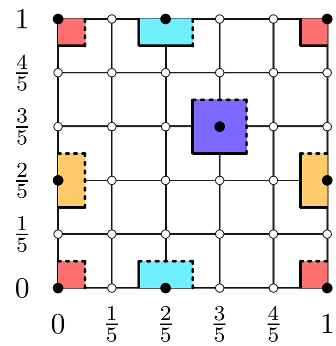

Figure 1: The above picture represents a square lattice (L_5) of spacing $\frac{1}{5}$ by circles and connecting lines. All points in the blue square $I_{\left(\frac{3}{5},\frac{3}{5}\right)} := \left[\frac{5}{10},\frac{7}{10}\right) \times \left[\frac{5}{10},\frac{7}{10}\right) \subset \mathbb{T}^2$ are associated with the grid point $\left(\frac{3}{5},\frac{3}{5}\right)$ (black dot). Thus, for all $\boldsymbol{x} \in I_{\left(\frac{3}{5},\frac{3}{5}\right)}$, it turns out that $|C_{\mathcal{N}}(\boldsymbol{x})\rangle = |\,(3,3)\rangle \in \mathcal{H}_{\mathcal{N}}$.

Proposition 3.1

The family of LS $\{|C_{\mathcal{N}}(\boldsymbol{x})\}$ satisfies Properties 3.1.

Proof:

Measurability and normalization are straightforward.

Completeness can be expressed as

$$\mathcal{N}\int_{\mathbb{T}^2}\mu(\mathrm{d}\boldsymbol{x})\,\langle \boldsymbol{\ell}\;|C_{\mathcal{N}}(\boldsymbol{x})\rangle\langle C_{\mathcal{N}}(\boldsymbol{x})|\;\boldsymbol{m}\rangle = \delta^{(N)}_{\boldsymbol{\ell},\boldsymbol{m}}, \qquad \forall \boldsymbol{\ell},\boldsymbol{m} \in (\mathbb{Z}/N\mathbb{Z})^2\;,$$

where we have introduced the periodic Kronecker delta, that is $\delta^{(N)}_{\boldsymbol{n},\boldsymbol{0}} = 1$ if and only if $\boldsymbol{n} \equiv \boldsymbol{0} \pmod N$. This is proved as follows:

$$\mathcal{N}\int_{\mathbb{T}^2}\mu(\mathrm{d}\boldsymbol{x})\,\langle\,\boldsymbol{\ell}\,|C_{\mathcal{N}}(\boldsymbol{x})\,\rangle\langle\,C_{\mathcal{N}}(\boldsymbol{x})\,|\,\boldsymbol{m}\,\rangle = \mathcal{N}\int_0^1 \mathrm{d}x_1 \int_0^1 \mathrm{d}x_2\;\langle\,\boldsymbol{\ell}\,|\,\hat{\boldsymbol{x}}_N\,\rangle\langle\,\hat{\boldsymbol{x}}_N\,|\,\boldsymbol{m}\,\rangle =$$

$$= \mathcal{N}\ \delta^{(N)}_{\ell_1\,,m_1}\ \delta^{(N)}_{\ell_2\,,m_2}\ \left[\int_0^1 \mathrm{d}x_1\, \delta^{(N)}_{\ell_1\,,\lfloor Nx_1+\frac12\rfloor}\right]\ \left[\int_0^1 \mathrm{d}x_2\ \ \delta^{(N)}_{\ell_2\,,\lfloor Nx_2+\frac12\rfloor}\right]$$

$$= \mathcal{N}\ \left(\delta^{(N)}_{\ell_1\,,m_1}\ \delta^{(N)}_{\ell_2\,,m_2}\right)\ \left[\int_{\frac{\ell_1-\frac12}{N}}^{\frac{\ell_1+\frac12}{N}} \mathrm{d}x_1\right]\ \left[\int_{\frac{\ell_2-\frac12}{N}}^{\frac{\ell_2+\frac12}{N}} \mathrm{d}x_2\right] = N^2\ \delta^{(N)}_{\boldsymbol{\ell},\boldsymbol{m}}\ \frac{1}{N^2} = \delta^{(N)}_{\boldsymbol{\ell},\boldsymbol{m}}\ \cdot$$

Localization comes as follows: from Definition 3.2 (see Remark 3.1 and Figure 1), it turns out that $|C_{\mathcal{N}}(\boldsymbol{x})\rangle$ is orthogonal to every basis element labeled by a point of L_N whose toral distance $d_{\mathbb{T}^2}$ (see Definition (3.1)) from $\boldsymbol{x}$ is greater than $\frac{1}{N\sqrt{2}}$. As a consequence, the quantity $\langle C_{\mathcal{N}}(\boldsymbol{x}), C_{\mathcal{N}}(\boldsymbol{y})\rangle = 0$ if the distance on the torus between $\boldsymbol{x}$ and $\boldsymbol{y}$ is greater than $\frac{\sqrt{2}}{N}$. Thus, given $d_0 > 0$, it is sufficient to choose $N_0(\epsilon, d_0) > \sqrt{2}/d_0$, to have

$$N > N_0(\epsilon, d_0) \Longrightarrow \mathcal{N}\ \langle C_{\mathcal{N}}(\boldsymbol{x}), C_{\mathcal{N}}(\boldsymbol{y})\rangle = 0\ \cdot \qquad \blacksquare$$

Remarks 3.2

(1) The last result in the previous Proposition amounts to an even stronger localization property than property 3.1.4; this is due to our particular choice of Lattice States, which, as we shall see, is suited to the task of controlling Sawtooth Maps. In general, one can hardly hope to achieve orthogonality and must be content with the weaker localization condition 3.1.4.

(2) Although the set of LS of Definition 3.2 fulfill Properties 3.1, which are typical of Coherent States, LS differ from them in that the context we are considering is commutative. In spite of this, it is convenient to adopt the formalism of Quantum Mechanics; in particular the set of LS is interpreted as a Hilbert orthonormal basis of Dirac kets, whose corresponding projectors form a partition of unit into indicator functions having support on small squares of the torus, as in Figure 1, whose sides scales as $\frac{1}{N}\ \cdot$

3.2. Anti–Wick Discretization and its continuous limit on $\mathbb{T}^2$

In order to study the continuous limit and, more generally, the quasi–continuous behaviour of $\left(\mathcal{D}_{\mathcal{N}}, \tau_{\mathcal{N}}, \Theta_{\mathcal{N}}\right)$ when $N \to \infty$, we follow the semi–classical technique known as Anti–Wick quantization. The other standard quantization technique, namely the Weyl procedure, despite being more straightforward and less technically heavy, is nevertheless more suited to smooth spaces of functions and was indeed instrumental in the study of discretized Cat Maps [14]. Instead, in our case, the Anti–Wick procedure is a better choice due to the discontinuous character of the dynamics, as it will clearly appear in the next Section.

We start choosing concrete discretization/de–discretization *-morphisms.

Definitions 3.3

Given the family $\{|C_{\mathcal{N}}(\boldsymbol{x})\rangle\}$ of Lattice States in $\mathcal{H}_{\mathcal{N}}$, the Anti-Wick–like discretization scheme (AW, for short) will be described by a one parameter family of (completely) positive unital map $\mathcal{J}_{\mathcal{N},\infty} : L^\infty_\mu\left(\mathbb{T}^2\right) \to \mathcal{D}_{\mathcal{N}}$

$$L^\infty_\mu\left(\mathbb{T}^2\right) \ni f \mapsto \mathcal{N}\int_{\mathbb{T}^2} \mu(\mathrm{d}\boldsymbol{x})\, f(\boldsymbol{x})\, |C_{\mathcal{N}}(\boldsymbol{x})\rangle\langle C_{\mathcal{N}}(\boldsymbol{x})| =: \mathcal{J}_{\mathcal{N},\infty}(f) \in \mathcal{D}_{\mathcal{N}} \quad .$$

The corresponding de–discretization operation will be described by the (completely) positive unital map $\mathcal{J}_{\infty,\mathcal{N}} : \mathcal{D}_{\mathcal{N}} \to L^\infty_\mu\left(\mathbb{T}^2\right)$

$$\mathcal{D}_{\mathcal{N}} \ni X \mapsto \langle C_{\mathcal{N}}(\boldsymbol{x}), X\, C_{\mathcal{N}}(\boldsymbol{x})\rangle =: \mathcal{J}_{\infty,\mathcal{N}}(X)(\boldsymbol{x}) \in L^\infty_\mu\left(\mathbb{T}^2\right) \quad .$$

Remarks 3.3

i. Both maps are identity preserving (unital) because of the conditions satisfied by the family of Lattice States and are completely positive, since both $L^\infty_\mu\left(\mathbb{T}^2\right)$ and $\mathcal{D}_{\mathcal{N}}$ are commutative algebras. One can also check that:

$$\left\|\mathcal{J}_{\infty,\mathcal{N}} \circ \mathcal{J}_{\mathcal{N},\infty}(g)\right\|_\infty \leq \|g\|_\infty, \quad g \in L^\infty_\mu\left(\mathbb{T}^2\right) \ \cdot$$

ii. Definition 3.3 yields $\tau_{\mathcal{N}} \circ \mathcal{J}_{\mathcal{N},\infty} = \omega_\mu$, with $\tau_{\mathcal{N}}$ given in (3).

In Appendix A, more operative details are presented, whereas in the following we prove some simple properties that incorporate minimal requests for rigorously defining the sense in which the discrete dynamical systems $\left(\mathcal{D}_{\mathcal{N}}, \tau_{\mathcal{N}}, \Theta_{\mathcal{N}}\right)$ tends to $\left(L^\infty_\mu\left(\mathbb{T}^2\right), \omega_\mu, \Theta\right)$, when $\frac{1}{N} \to 0$.

Proposition 3.2

(1) For all $f \in L^\infty_\mu\left(\mathbb{T}^2\right)$ and $X \in \mathcal{D}_{\mathcal{N}}$,

$$\omega_\mu\left(\overline{g}\ \mathcal{J}_{\infty,\mathcal{N}}\left(X\right)\right) = \tau_{\mathcal{N}}\big(\mathcal{J}_{\mathcal{N},\infty}(g)^* X\big) \ ;$$

(2) For all $f, g \in L^\infty_\mu\left(\mathbb{T}^2\right)$

$$\lim_{N\to\infty} \tau_{\mathcal{N}}\big(\mathcal{J}_{\mathcal{N},\infty}(f)^* \mathcal{J}_{\mathcal{N},\infty}(g)\big) = \omega_\mu(\overline{f}g) = \int_{\mathbb{T}^2} \mu(\mathrm{d}\boldsymbol{x})\,\overline{f(\boldsymbol{x})}g(\boldsymbol{x}).$$

(3) For all $X \in \mathcal{D}_{\mathcal{N}}$, and for all $N \in \mathbb{N}^+$,

$$\mathcal{J}_{\mathcal{N},\infty} \circ \mathcal{J}_{\infty,\mathcal{N}}\ (X) = X\ ;$$

(4) For all $f \in L^\infty_\mu\left(\mathbb{T}^2\right)$

$$\lim_{N\to\infty} \mathcal{J}_{\infty,\mathcal{N}} \circ \mathcal{J}_{\mathcal{N},\infty}(f) = f \quad \mu - \text{a.e.}$$

Proof:

The first two statements in the above Proposition directly follow from Definitions 3.3 together with (6); the latter two are equivalent and their proof can be found in [25], the only difference being the dimension $\mathcal{N}$ of the Hilbert space $\mathcal{H}_{\mathcal{N}}$, here $\mathcal{N} = N^2$, there $\mathcal{N} = N$. ∎

Remark 3.4

Properties 1 and 2 in the previous Proposition show how (GNS) scalar products in the discrete, respectively continuous limit, are related; properties 3 and 4 concern instead the direct–inverse relations between the discretization and the de–discretization maps.

4. Discretization of the Dynamics

4.1. Classical description of Sawtooth Maps

We shall now focus on a special class of automorphisms of the torus, namely the Sawtooth Maps [16,17] (SM for short), that is on triples $(\mathbb{T}^2, \mu, S_\alpha)$ where

$$\begin{aligned} S_\alpha \begin{pmatrix} x_1 \\ x_2 \end{pmatrix} &= \begin{pmatrix} 1+\alpha & 1 \\ \alpha & 1 \end{pmatrix} \begin{pmatrix} \langle x_1 \rangle \\ x_2 \end{pmatrix} \quad (\mathrm{mod}\ 1)\ , \quad \alpha \in \mathbb{R} \\ &= \begin{pmatrix} \langle (1+\alpha)\langle x_1 \rangle + x_2 \rangle \\ \langle \alpha \langle x_1 \rangle + x_2 \rangle \end{pmatrix} \end{aligned} \tag{7}$$

Remarks 4.1

i. In the following, a point $\boldsymbol{x}$ of the torus, will correspond to an equivalence class of $\mathbb{R}^2$ points whose coordinates differ by integer values;

ii. without the fractional part, (7) is not well defined on $\mathbb{T}^2$ for not–integer α; indeed, the same point $\boldsymbol{x} = \boldsymbol{x} + \boldsymbol{n} \in \mathbb{T}^2, \boldsymbol{n} \in \mathbb{Z}^2$, would have (in general) $S_\alpha(\boldsymbol{x}) \neq S_\alpha(\boldsymbol{x}+\boldsymbol{n})$. Of course, $\langle\cdot\rangle$ is not necessary when $\alpha \in \mathbb{Z}$;

iii. the Lebesgue measure on $\mathbb{T}^2$ is *invariant* for all $\alpha \in \mathbb{R}$;

iv. if $\alpha \notin \mathbb{Z}$, the S_α are known as Sawtooth Maps;

v. when $\alpha \in \mathbb{Z}$, we shall write T_α instead of S_α. $T_1 = \left(\begin{smallmatrix} 2 & 1 \\ 1 & 1 \end{smallmatrix}\right)$ is the Arnold Cat Map [6]. In general, $T_1 \in \{T_\alpha\}_{\alpha\in\mathbb{Z}} \subset \mathrm{SL}_2(\mathbb{Z}) \subset \mathrm{GL}_2(\mathbb{Z}) \subset \mathrm{M}_2(\mathbb{Z})$ where $\mathrm{M}_2(\mathbb{Z})$ is the subset of 2×2 matrices with integer entries, $\mathrm{GL}_2(\mathbb{Z})$ the subset of invertible matrices and $\mathrm{SL}_2(\mathbb{Z})$ the subset of matrices with determinant one: the dynamics generated by $T_\alpha \in \mathrm{SL}_2(\mathbb{Z})$ is called *Unimodular Group* [6] (UMG for short);

vi. after identifying $\boldsymbol{x}$ with canonical coordinates (q,p) and imposing the (mod 1) condition on both of them, the above dynamics reads

$$\begin{cases} q' &= q + p' \\ p' &= p + \alpha\langle q \rangle \end{cases} \quad (\mathrm{mod}\ 1)\ \cdot \tag{8}$$

This is nothing but the Chirikov Standard Map [3] in which $-\frac{1}{2\pi}\sin(2\pi q)$ is replaced by $\langle q \rangle$. The dynamics in (8) can also be thought of as generated by the (singular) Hamiltonian

$$H(q,p,t) = \frac{p^2}{2} - \alpha\,\frac{\langle q\rangle^2}{2}\,\delta_p(t),$$

where $\delta_p(t)$ is the periodic Dirac delta which makes the potential act through periodic kicks with period 1 [26];

vii. Sawtooth Maps are invertible and the inverse is given by the expression

$$\begin{aligned} S_\alpha^{-1}\begin{pmatrix} x_1 \\ x_2 \end{pmatrix} &= \begin{pmatrix} 1 & 0 \\ -\alpha & 1 \end{pmatrix}\left\langle \begin{pmatrix} 1 & -1 \\ 0 & 1 \end{pmatrix}\begin{pmatrix} x_1 \\ x_2 \end{pmatrix}\right\rangle \pmod 1 \\ &= \begin{pmatrix} \langle x_1 - x_2\rangle \\ \langle\langle x_2\rangle - \alpha\,\langle x_1 - x_2\rangle\rangle \end{pmatrix} \end{aligned} \tag{9}$$

or, in other words,

$$\begin{cases} q &= \quad q' - p' \\ p &= -\alpha\, q\ + p' \end{cases} \pmod 1 .$$

It can indeed be checked that $S_\alpha\left(S_\alpha^{-1}(\boldsymbol{x})\right) = S_\alpha^{-1}\left(S_\alpha(\boldsymbol{x})\right) = \boldsymbol{x},\ \forall \boldsymbol{x} \in \mathbb{T}^2$. Further, S_α^{-1} preserves the Lebesgue measure on $\mathbb{T}^2$.

We now list a set of properties [16–18] of Sawtooth Maps that will be used in the following

Properties 4.1 (of Sawtooth Maps)

(1) Sawtooth Maps $\{S_\alpha\}$ are *discontinuous* on the subset $\gamma_0 := \{\boldsymbol{x} = (0,p)\,,\ p \in \mathbb{T}\} \in \mathbb{T}^2$: two points close to γ_0, $A := (\varepsilon, p)$ and $B := (1-\varepsilon, p)$, have images that differ, in the $\varepsilon \to 0$ limit, by a vector $d^{(1)}_{S_\alpha}(A,B) = (\alpha,\alpha) \pmod 1$.

(2) Inverse Sawtooth Maps $\{S_\alpha^{-1}\}$ are *discontinuous* on the subset $\gamma_{-1} := S_\alpha(\gamma_0) = \{\boldsymbol{x} = (p,p)\,,\ p \in \mathbb{T}\} \in \mathbb{T}^2$: two points close to γ_{-1}, namely $A := (p+\varepsilon, p-\varepsilon)$ and $B := (p-\varepsilon, p+\varepsilon)$, have images that differ, in the $\varepsilon \to 0$ limit, by a vector $d^{(1)}_{S_\alpha^{-1}}(A,B) = (0,\alpha) \pmod 1$.

(3) The maps T_α and T_α^{-1} are *continuous*: $\alpha \in \mathbb{Z} \Longrightarrow d^{(1)}_{T_\alpha}(A,B) = d^{(1)}_{T_\alpha^{-1}}(A,B) = (0,0) \pmod 1$.

(4) The eigenvalues of the matrix $S_\alpha = \left(\begin{smallmatrix} 1+\alpha & 1 \\ \alpha & 1 \end{smallmatrix}\right)$ are $\left(\alpha + 2 \pm \sqrt{(\alpha+2)^2 - 4}\right)/2$. They are conjugate complex numbers if $\alpha \in [-4, 0]$, whereas one eigenvalue

$\lambda > 1$ if $\alpha \notin [-4, 0]$. In this case, distances are stretched along the direction of the eigenvector $|\boldsymbol{e}_+\rangle$, $S_\alpha|\boldsymbol{e}_+\rangle = \lambda|\boldsymbol{e}_+\rangle$, contracted along that of $|\boldsymbol{e}_-\rangle$, $S_\alpha|\boldsymbol{e}_-\rangle = \lambda^{-1}|\boldsymbol{e}_-\rangle$: $\log\lambda$ is a (positive) *Lyapunov exponent*.
For such α's all periodic points are hyperbolic [18].

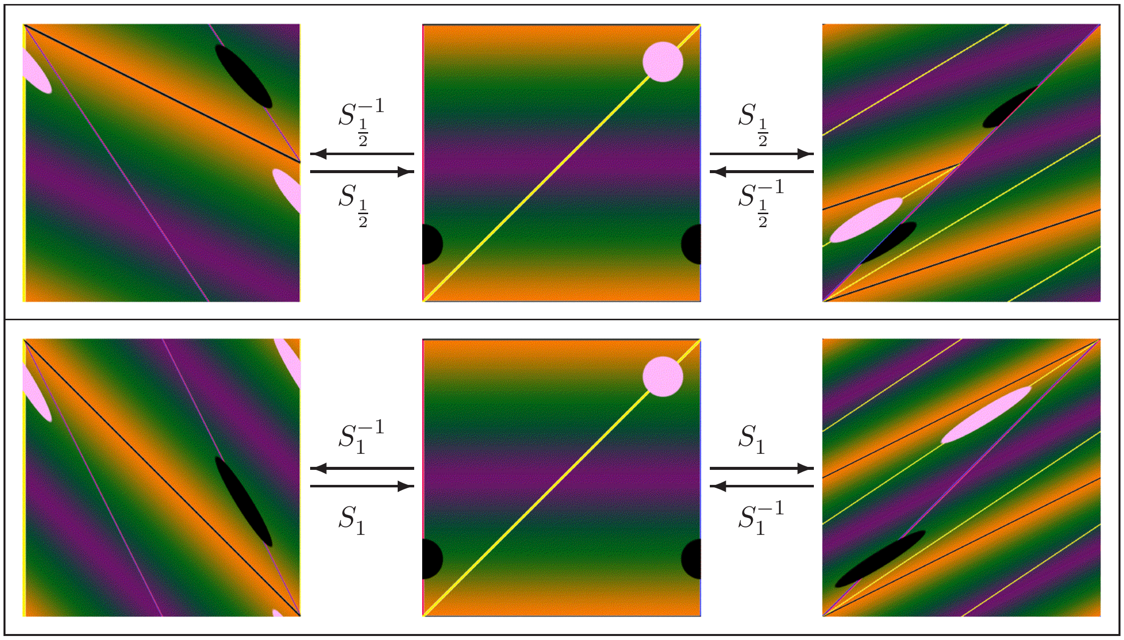

Figure 2: In the upper row, we depict the effects of the discontinuities of a SM with $\alpha = \frac{1}{2}$; the picture in the middle shows the discontinuity lines γ_0 and γ_{-1}, whereas those on the right and left show how they evolve backward and forward in time. The different parallel bands help the reader to figure out the toral periodicity and the discontinuous character of the map, also highlighted by the aperiodic splits of two spots. Further, for sake of comparison, the lower row presents the same case of the upper one but for the continuous dynamics ($\alpha = 1$).

Remarks 4.2

Because of the presence of the fractional part in (7) and (9), we have to distinguish the action of S_α and S_α^{-1} from a mere matrix action. We shall adopt the following notations:

i. With S_α the matrix $\left(\begin{smallmatrix}1+\alpha & 1\\ \alpha & 1\end{smallmatrix}\right)$ in Property 4.1.4, the expression $S_\alpha(\boldsymbol{x})$ will denote the action represented by (7), whereas $S_\alpha \cdot \boldsymbol{x}$ will denote the matrix action of S_α on the vector $\boldsymbol{x}$.

ii. When the dynamics arises from the action of the UMG (see Remark 4.1.v.), so, in particular, when $\{T_\alpha\}_{\alpha\in\mathbb{Z}}$ is the family of toral automorphisms, equation (7) assumes the simpler form $T_\alpha(\boldsymbol{x}) = T_\alpha \cdot \boldsymbol{x} \pmod 1$.

iii. Analogously, expressions like $T_\alpha \cdot \boldsymbol{x}$, $T_\alpha^{\mathrm{tr}} \cdot \boldsymbol{x}$, $T_\alpha^{-1} \cdot \boldsymbol{x}$ and $\left(T_\alpha^{\mathrm{tr}}\right)^{-1} \cdot \boldsymbol{x}$, will denote the actions by T_α itself, its transposed, its inverse and the inverse of the transposed, respectively.

4.2. Algebraic description of continuous and discretized Sawtooth Maps

In this Section we make use of the commutative (Von Neumann) algebra $L^\infty_\mu\left(\mathbb{T}^2\right)$ introduced in Section 2 and consider the algebraic description of Sawtooth Maps by triples $\left(L^\infty_\mu\left(\mathbb{T}^2\right), \omega_\mu, \Theta_\alpha\right)$, where ω_μ has been defined in (1) and $\Theta_\alpha : L^\infty_\mu\left(\mathbb{T}^2\right) \mapsto L^\infty_\mu\left(\mathbb{T}^2\right)$ is the discrete–time dynamics generated as follows:

$$\Theta_\alpha(f)(\boldsymbol{x}) := f(S_\alpha(\boldsymbol{x})) \quad , \quad \alpha \in \mathbb{R} \cdot$$

The maps Θ_α^j, $j \in \mathbb{Z}$ are automorphisms of $L^\infty_\mu\left(\mathbb{T}^2\right)$ and leave the state ω_μ invariant.

Our aim is now to define a suitable discrete evolution $\Theta_{\mathcal{N},\alpha}$ on $\mathcal{D}_\mathcal{N}$, such that the discretized triplets $\left(\mathcal{D}_\mathcal{N}, \tau_\mathcal{N}, \Theta_{\mathcal{N},\alpha}\right)$ converge to the continuous SM.

We start by introducing two different kinds of maps: the first ones, $U_\alpha^{\pm j}$, $j \in \mathbb{Z}$, are defined on the torus $\mathbb{T}^2\left([0,N)^2\right)$, namely $[0,N) \times [0,N) \pmod N$, and given by

$$\begin{aligned}
\mathbb{T}^2\left([0,N)^2\right) \ni \boldsymbol{x} \mapsto\ & U_\alpha^0(\boldsymbol{x}) := \boldsymbol{x} \\
&= N\, S_\alpha^0\left(\frac{\boldsymbol{x}}{N}\right) \in \mathbb{T}^2\left([0,N)^2\right) \ , && \text{(10a)} \\
\mathbb{T}^2\left([0,N)^2\right) \ni \boldsymbol{x} \mapsto\ & U_\alpha^{\pm1}(\boldsymbol{x}) := N\, S_\alpha^{\pm1}\left(\frac{\boldsymbol{x}}{N}\right) \in \mathbb{T}^2\left([0,N)^2\right) \ , && \text{(10b)} \\
\mathbb{T}^2\left([0,N)^2\right) \ni \boldsymbol{x} \mapsto\ & U_\alpha^{\pm j}(\boldsymbol{x}) := \underbrace{U_\alpha^{\pm1}(\,U_\alpha^{\pm1}(\cdots U_\alpha^{\pm1}(\,U_\alpha^{\pm1}(}_{j \text{ times}}\boldsymbol{x}\,))\cdots))\ , \quad j \in \mathbb{N}^+ \ , \\
&= N\, S_\alpha^{\pm j}\left(\frac{\boldsymbol{x}}{N}\right) \in \mathbb{T}^2\left([0,N)^2\right) \ \cdot && \text{(10c)}
\end{aligned}$$

The second class consists of maps $V_\alpha^{\pm j}$ from $\mathbb{T}^2\left([0,N)^2\right)$ onto its subset $(\mathbb{Z}/N\mathbb{Z})^2$, whose actions are as follows

$$\mathbb{T}^2\left([0,N)^2\right) \ni \boldsymbol{x} \mapsto \quad V_\alpha^0(\boldsymbol{x}) := \lfloor \boldsymbol{x} \rfloor$$

$$= \pm \left\lfloor \pm U_\alpha^0(\lfloor \boldsymbol{x} \rfloor)\right\rfloor \in (\mathbb{Z}/N\mathbb{Z})^2 \ , \tag{11a}$$

$$\mathbb{T}^2\left([0,N)^2\right) \ni \boldsymbol{x} \mapsto V_\alpha^{\pm 1}(\boldsymbol{x}) := \pm \left\lfloor \pm U_\alpha^{\pm 1}(\lfloor \boldsymbol{x} \rfloor)\right\rfloor \in (\mathbb{Z}/N\mathbb{Z})^2 \ , \tag{11b}$$

$$\mathbb{T}^2\left([0,N)^2\right) \ni \boldsymbol{x} \mapsto V_\alpha^{\pm j}(\boldsymbol{x}) := \underbrace{V_\alpha^{\pm 1}(\, V_\alpha^{\pm 1}(\cdots V_\alpha^{\pm 1}(\, V_\alpha^{\pm 1}(}_{j\ \text{times}}\lfloor \boldsymbol{x} \rfloor\,)\,)\cdots)\,)\ , \quad j \in \mathbb{N}^+ \ ,$$

$$= \underbrace{\pm\lfloor \pm U_\alpha^{\pm 1}(\pm\lfloor \pm U_\alpha^{\pm 1}(\cdots \pm \lfloor \pm U_\alpha^{\pm 1}(\pm\lfloor \pm U_\alpha^{\pm 1}(}_{j\ \text{times}}\lfloor \boldsymbol{x} \rfloor\,)\rfloor\,)\rfloor \cdots)\rfloor\,)\rfloor \in (\mathbb{Z}/N\mathbb{Z})^2 \cdot \tag{11c}$$

Remark 4.3

The maps U_α^j are extensions of the S_α^j on the enlarged torus $\mathbb{T}^2\left([0,N)^2\right)$; however, they do not map the lattice L_N into itself, therefore we are forced to use the maps V_α^j to define a consistent discretized dynamics.

Definition 4.1

$\Theta_{\mathcal{N},\alpha}$ will denote the map:

$$\mathcal{D}_{\mathcal{N}} \ni X \mapsto \Theta_{\mathcal{N},\alpha}(X) := \sum_{\boldsymbol{\ell} \in (\mathbb{Z}/N\mathbb{Z})^2} X_{V_\alpha(\boldsymbol{\ell}),V_\alpha(\boldsymbol{\ell})}\, |\boldsymbol{\ell}\rangle\langle\boldsymbol{\ell}| \in \mathcal{D}_{\mathcal{N}} \cdot \tag{12}$$

$\Theta_{\mathcal{N},\alpha}$ is a *-automorphism of $\mathcal{D}_{\mathcal{N}}$; indeed, the map

$$(\mathbb{Z}/N\mathbb{Z})^2 \ni \boldsymbol{\ell} \longmapsto V_\alpha(\boldsymbol{\ell}) \in (\mathbb{Z}/N\mathbb{Z})^2$$

is a bijection, so that (12) can be rewritten in the more convenient form

$$\begin{aligned}
\Theta_{\mathcal{N},\alpha}(X) &= \sum_{\boldsymbol{\ell} \in (\mathbb{Z}/N\mathbb{Z})^2} X_{V_\alpha(\boldsymbol{\ell}),V_\alpha(\boldsymbol{\ell})}\, |\boldsymbol{\ell}\rangle\langle\boldsymbol{\ell}| = \\
&= \sum_{V_\alpha^{-1}(\boldsymbol{s}) \in (\mathbb{Z}/N\mathbb{Z})^2} X_{\boldsymbol{s},\boldsymbol{s}}\, \left|V_\alpha^{-1}(\boldsymbol{s})\right\rangle\left\langle V_\alpha^{-1}(\boldsymbol{s})\right| = \\
\text{(see Remark 4.4.iii. below)} \quad &= W_{\alpha,N}\left(\sum_{\substack{\text{all equiv.}\\ \text{classes}}} X_{\boldsymbol{s},\boldsymbol{s}}\, |\boldsymbol{s}\rangle\langle\boldsymbol{s}|\right) W_{\alpha,N}^* = \qquad (13) \\
&= W_{\alpha,N}\ X\ \ W_{\alpha,N}^* \ ,
\end{aligned}$$

where the operators $W_{\alpha,N}$, defined by linearly extending the maps

$$\mathcal{H}_{\mathcal{N}} \ni \left|\boldsymbol{\ell}\right\rangle \longmapsto W_{\alpha,N}\left|\boldsymbol{\ell}\right\rangle := \left|V_\alpha^{-1}\left(\boldsymbol{\ell}\right)\right\rangle \in \mathcal{H}_{\mathcal{N}} \cdot \tag{14}$$

to $\mathcal{H}_{\mathcal{N}}$, are unitary: $W^*_{\alpha,N}\left|\boldsymbol{\ell}\right\rangle := \left|V_\alpha\left(\boldsymbol{\ell}\right)\right\rangle$.

For the same reason the state $\tau_{\mathcal{N}}$ is $\Theta_{\mathcal{N},\alpha}$–invariant and V_α is invertible too.

Note that $\Theta^j_{\mathcal{N},\alpha} := \underbrace{\Theta_{\mathcal{N},\alpha} \circ \cdots \circ \Theta_{\mathcal{N},\alpha}}_{j \text{ times}}$ is implemented by $V^j_\alpha\left(\boldsymbol{\ell}\right)$ given in (11c).

Remarks 4.4

i. The double $\pm$ sign in front and within every floor function in equations (11) is needed in order to have $V_\alpha^{\pm j}(V_\alpha^{\mp j}(\boldsymbol{x})) = V_\alpha^0(\boldsymbol{x})$ (the identity when $\boldsymbol{x} \in (\mathbb{Z}/N\mathbb{Z})^2$); the reason is that, in general, $\lfloor -x \rfloor \neq -\lfloor x \rfloor$, for $x \notin \mathbb{Z}$ (see [27]).

ii. When $\alpha \in \mathbb{Z}$, $(\mathbb{Z}/N\mathbb{Z})^2 \ni \boldsymbol{\ell} \longmapsto V_\alpha\left(\boldsymbol{\ell}\right) = T_\alpha \cdot \boldsymbol{\ell} \in (\mathbb{Z}/N\mathbb{Z})^2$, namely the action of the map V_α becomes that of a matrix (mod N). Moreover, in that case, U_α and V_α coincide.

iii. Since $\boldsymbol{\ell} \longmapsto V_\alpha\left(\boldsymbol{\ell}\right)$ is a bijection, in (13) one can sum over the equivalence classes.

5. Continuous limit of the dynamics

One of the main issues in the semi-classical analysis is to compare if and how the quantum and classical time evolutions mimic each other when a suitable quantization parameter goes to zero.

In this article we are instead considering the possible agreement between the dynamics of continuous classical systems and that of a class of discrete approximants. In practice, in our case, we will study the difference

$$\Theta^j_\alpha - \mathcal{J}_{\infty,\mathcal{N}} \circ \Theta^j_{\mathcal{N},\alpha} \circ \mathcal{J}_{\mathcal{N},\infty} \tag{15}$$

which represents how much the discrete dynamics at timestep j differs from the continuous one at the same timestep.

For quantum systems, whose classical limit is chaotic, the situation is strikingly different from those with regular classical limit. In the former case, classical and quantum mechanics agree, that is a difference as in (15) is negligible, only over times j which scale logarithmically (and not as a power law) in the quantization parameter.

As we shall see, such a type of scaling is not exclusively related with non–commutativity; in fact, the quantization–like procedure developed so far, exhibits a similar behavior when $N \to \infty$ and we recover $\left(L^\infty_\mu\left(\mathbb{T}^2\right), \omega_\mu, \Theta_\alpha\right)$ as a continuous limit of $\left(\mathcal{D}_\mathcal{N}, \tau_\mathcal{N}, \Theta_{\mathcal{N},\alpha}\right)$.

5.1. Continuous limit for Sawtooth Maps

Later on we shall show that the difference in (15) goes to zero in a suitable topology; for the moment we just note that the major difficulties in the proof are due to the discontinuous character of the fractional part that appears in (7).

It is therefore important to briefly discuss the discontinuities of the maps S_α [16–18].

As already noted in Property 4.1.1, S_α is discontinuous on the circle γ_0; therefore S^n_α will be discontinuous on the preimages

$$\gamma_m := S_\alpha^{-m}\left(\gamma_0\right) \quad \text{for} \quad 0 \leqslant m < n \ , \tag{16a}$$

whereas the discontinuities of S_α^{-n} lie on the sets

$$\gamma_{-m} := S_\alpha^{m}\left(\gamma_0\right) \quad \text{for} \quad 0 < m \leqslant n \ \cdot \tag{16b}$$

Apart from γ_{-1}, whose projection on the $[0,1)^2$ square is its diagonal (see Fig. 5), each set of the type γ_m (for γ_{-m} the argument is similar) is the (disjoint) union of segments parallel to each other whose endpoints lie either on the same segment belonging to γ_p, $p < m$, or on two different segments belonging to γ_p and $\gamma_{p'}$, with $p' \leqslant p < m$ [17].
It proves convenient to introduce the *discontinuity set* of S^n_α,

$$\mathbb{T}^2 \supset \Gamma_n := \bigcup_{p=0}^{n-1} \gamma_p \ , \tag{17}$$

and its complementary set, $G_n := \mathbb{T}^2 \setminus \Gamma_n$.

We now enlarge the previous definition from continuous Sawtooth Maps, to discretized ones.

Definitions 5.1

We shall call "segment", and denote it by (A, B), the shortest curve joining $A, B \in \mathbb{T}^2$, by $l(\gamma_p)$ the length of the curve γ_p and by

$$\overline{\gamma}_p(\varepsilon) := \left\{ \boldsymbol{x} \in \mathbb{T}^2 \;\middle|\; d_{\mathbb{T}^2}(\boldsymbol{x}, \gamma_p) \leqslant \varepsilon \right\} \tag{18}$$

the strip around γ_p of width ε, where the distance $d_{\mathbb{T}^2}(\cdot, \cdot)$ on the torus has been introduced in Definition 3.1.

Further, we shall denote by

$$\overline{\Gamma}_n(\varepsilon) := \bigcup_{p=0}^{n-1} \overline{\gamma}_p(\varepsilon) \tag{19}$$

the union of the strips up to $p = n - 1$ and by $G_n^N(\varepsilon)$ the subset of points

$$G_n^N(\varepsilon) := \left\{ \boldsymbol{x} \in \mathbb{T}^2 \;\middle|\; \frac{\hat{\boldsymbol{x}}_N}{N} \notin \overline{\Gamma}_n(\varepsilon) \right\} \ , \tag{20}$$

where the lattice points $\hat{\boldsymbol{x}}_N$ have been introduced in Definition 3.2.

As already observed, in order to prove that the discretized SM tend to continuous SM when $N \to \infty$, the main problem is to control the discontinuities. It proves convenient to subdivide the lattice points in a *good* and a *bad* set and show that, on the former, $V_\alpha^q \simeq U_\alpha^q$, at least on a certain time–scale (see Remark 4.3). This will not turn out to be true for the bad set, however we shall show that the latter tends with N to a set of zero Lebesgue measure and thus becomes ineffective.

Following this strategy, we shall concretely show that the difference (15) goes to zero with $N \to \infty$ in the strong topology over the Hilbert space $L^2_\mu(\mathbb{T}^2)$. More precisely, we have the following theorem

Theorem 1

Let $(\mathcal{D}_\mathcal{N}, \tau_\mathcal{N}, \Theta_{\mathcal{N},\alpha})$ be a sequence of discretized SM as defined in Section 4: for all $\gamma > 3$,

$$\forall f \in L^\infty_\mu(\mathbb{T}^2) \quad , \quad \underset{\substack{j,N \to \infty \\ j < \frac{1}{\gamma} \frac{\log N}{\log \eta}}}{\text{s–lim}} \left(\Theta_\alpha^j - \mathcal{J}_{\infty,\mathcal{N}} \circ \Theta_{\mathcal{N},\alpha}^j \circ \mathcal{J}_{\mathcal{N},\infty} \right)(f) = 0 \quad , \tag{21}$$

where the limit is in the strong topology over the Hilbert space $L^2_\mu(\mathbb{T}^2)$ and $\eta > \sqrt{2}$ is the largest eigenvalue of the matrix $|S_\alpha| := \sqrt{S_\alpha^\dagger S_\alpha}$, with S_α defined in Property 4.1.4.

The previous Theorem indicates that the time limit and the continuous limit do not commute. In particular, the difference between the discretized dynamics and the continuous one can be made small by increasing N, while it becomes large beyond the time scale $j \simeq \frac{1}{\gamma}\frac{\log N}{\log \eta}$. This phenomenon is the same as in quantum chaos and points to discretization of phase space (in the traditional semi–classical treatment of quantum systems), rather than to non–commutativity, as the source of the so–called *logarithmic breaking time*. The constant γ is a *form factor*, which reflects the fine structure of the dynamics: for instance, in the case of quantum cat maps [25], $\gamma = 2$.

Remark 5.1

The parameter $\gamma > 3$ in Theorem 1 may seem overestimated if compared with the case of the quantum Cat Map, where $\gamma = 2$. As we shall see (in particular in the next Proposition 5.2), the upper bound for γ is dictated by the discontinuities of the Sawtooth Maps, and not by commutativity. The corresponding exponent assumes the lower value $\gamma > 1$ in the case of discretized Cat Maps, that include Sawtooth Maps with integer α. This result will be presented in a forthcoming paper [28], in which we study the breaking time $\tau_{\mathrm{B}}(N)$, here $\frac{1}{\gamma}\frac{\log N}{\log \eta}$, relative to the chaotic or non–chaotic properties of the dynamics. In particular, in the hyperbolic regime, the parameter $\log \eta$ of Theorem 1 is replaced by the Lyapunov exponent $\log \lambda$ whereas, in the elliptic regime, the two limits $j, N \longrightarrow \infty$ do commute and in the parabolic one, the breaking time is given by $\tau_{\mathrm{B}}(N) = N^{\frac{1}{\gamma}}$.

The proof of Theorem 1 consists of several steps, among which the most important is a property, satisfied by our choice of Lattice States, which we shall call *dynamical localization.*

We give a full proof that our choice of Lattice States satisfies such property, since it represents a natural request that should be fulfilled by any consistent discretization/de–discretization (quantization/de–quantization) scheme.

Remarks 5.2

(1) In analogy to the quantum case, Dynamical localization is what one expects from a good choice of states suited the study of the continuous limit:

in fact, it essentially amounts to asking that LS remain decently localized around the continuous trajectories while evolving with the corresponding discrete evolution. As we shall see this is the case only on logarithmic time–scales. Informally, when $N \to \infty$, the quantities

$$K_j(\boldsymbol{x},\boldsymbol{y}) := \langle C_{\mathcal{N}}(\boldsymbol{x}), W^j_{\alpha,N}\, C_{\mathcal{N}}(\boldsymbol{y})\rangle$$

should behave as if $\mathcal{N}|K_j(\boldsymbol{x},\boldsymbol{y})|^2 \simeq \delta(S^j_\alpha\, \boldsymbol{x} - \boldsymbol{y})$: this would make the discretization analogous to the notion of *regular quantization* described in Section V of [29]. Actually, with our choice of LS, the quantity $K_j(\boldsymbol{x},\boldsymbol{y})$ is a Kronecker delta.

(2) In quantum chaos, instead of seeking for the dynamical localization, one can study the *dynamical spreading* of Coherent States. Consider for instance the classical function f over the phase space, its corresponding quantum observable $\mathrm{Op}_\hbar(f)$ and a Coherent State $|C_\hbar(\boldsymbol{x})\rangle$ centred at the point $\boldsymbol{x}$. The time needed for the quantum mechanical expectation $\langle C_\hbar(\boldsymbol{x}), \mathrm{Op}_\hbar(f)\, C_\hbar(\boldsymbol{x})\rangle$ to converge to the average of f over a suitable invariant measure can be explicitly analyzed. Recent work [7, 9] shows that also this time scales logarithmically in $\hbar$, at least for the automorphisms on the 2–torus.

(3) The constraint $j \leq C \log \mathcal{N}$ is typical of *hyperbolic* behavior with Lyapunov exponent $\log\lambda$ and comes heuristically as follows: the expansion of an initial small distance δ can be exponential until the distance becomes the largest possible, namely $\delta\lambda^{T_{\mathrm{B}}} \simeq 1$. After discretization, the minimal distance gives $\delta = \frac{1}{N}$, therefore one estimates $T_{\mathrm{B}} \simeq \frac{\log N}{\log\lambda}$, which is called *breaking time* and sets the time–scale over which continuous and discretized dynamics mimic each other.

(4) In quantum chaos, the semi–classical analysis leads to an estimate of T_{B} exactly as above; further, the logarithmic dependence on $\hbar$ of T_{B} is a signature of the hyperbolic character of the classical limit. Conversely, if the classical limit is regular, then the time scale when quantum and classical behaviors are more or less indistinguishable goes as $\hbar^{-b}$, $b > 0$. Another interpretation of the breaking time is given in [8], where it is related to the shortest time needed for the system to transfer all scales $1 \geqslant \ell \geqslant \hbar$ down to the "quantum scale" $\hbar$. Indeed, this is the scale at which the differences among quantum and classical mechanics come up. Regarding the SM, the hyperbolic case corresponds to S_α with eigenvalue $\lambda > 1$, whereas the regular cases are the *elliptic* one (two complex eigenvalues) and the *parabolic*

one (only one eigenvalue = 1).

(5) The dynamical localization property has fruitfully been used in several quantum contexts [25]; however, to our knowledge, this is the first instance, though not properly quantal, where dynamical localization is fully exposed.

Before proceeding with the proof of Theorem 1, it is important to notice that in its statement the Lyapunov exponent $\log\lambda$ does not appear but $\log\eta$, instead; of course λ and η are related for λ is eigenvalue of S_α, and η of $\sqrt{S_\alpha^\dagger S_\alpha}$ (see Remark 5.1).

As will become clear during the proof, the use of η and not of λ is required by the discontinuous character of SM. In fact, the discontinuities do not allow us to control the difference between the n–th iterates of the discretized and the continuous dynamics, but instead force us to estimate that difference at each single time–step up to n and to put all the estimates together. In the single time–step estimate, independently of whether the map is continuous or not, one must use η, which coincides with λ only when the dynamical matrix S_α is symmetric. Indeed, Figure 3 shows that the eigenvalue η correctly describes how volumes behaves under a single application of the dynamics, whereas λ underestimates it. On the contrary, it is λ^n which asymptotically controls the stretching, whereas η^n largely overestimates it. In the regular elliptic case, where $\lambda = 0$ and $\eta \geqslant \sqrt{2}$, the use of η gives the impression of hyperbolic stretching, whereas the elliptic motion is confined: from the lower strip in Figure 3 it is apparent that such hyperbolicity is spurious.

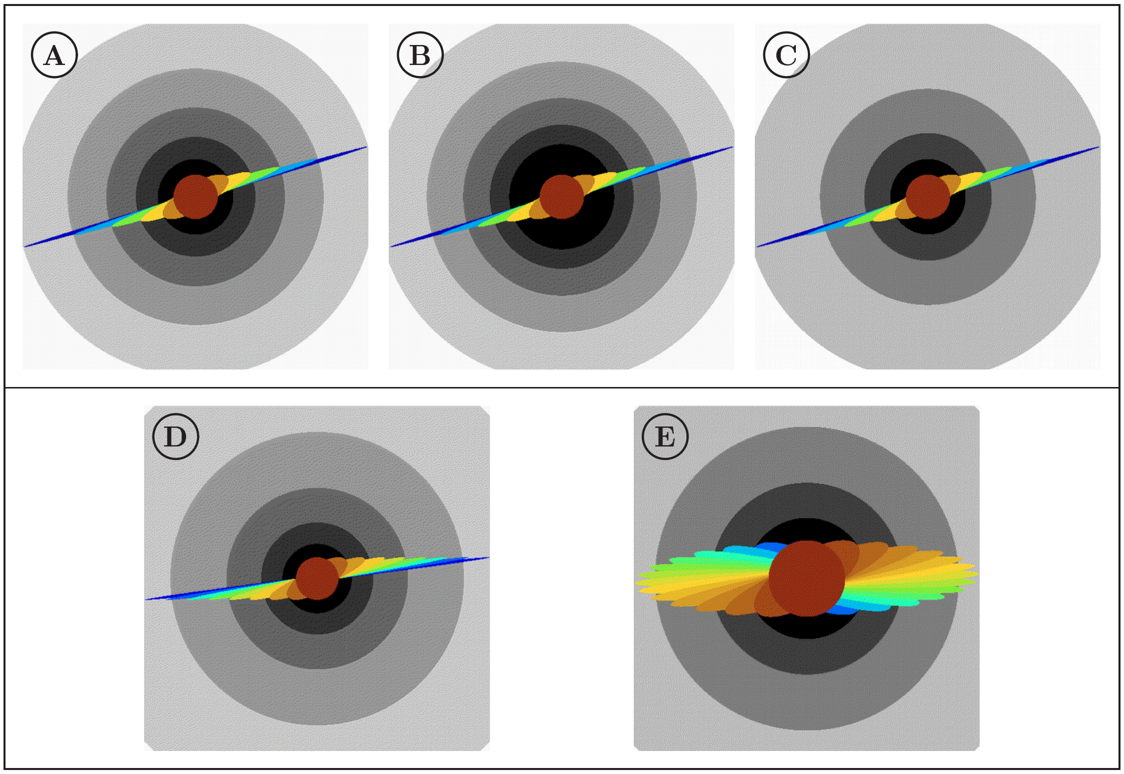

Figure 3: In Plots **A**, **B** and **C** we compare the estimates of the (maximum) stretching given by the action of the SM $S_{1/10}$ and its temporal iterates $S^n_{1/10}$ $(n \leqslant 5)$ given by λ, respectively η, on a small ball $B^0_{\boldsymbol{v}}$ of radius $\boldsymbol{v}$, centered in $\left(\frac{1}{2}, \frac{1}{2}\right) \in \mathbb{T}^2$. The five evolved images of the ball, namely $\{B^n_{\boldsymbol{v}}\ ,\ 1 < n \leqslant 5\}$, are plotted together with $B^0_{\boldsymbol{v}}$, using different colors. In **A** we surround every evolved ball $B^n_{\boldsymbol{v}}$ with the smallest circle containing it. We compare that plot with **B** and **C**, in which the surrounding circles have radii proportional to $\lambda^n \boldsymbol{v}$, respectively $\eta^n \boldsymbol{v}$; in both cases the correct radii of **A** are overestimated although, on the long run, circles in **B** provide a good approximation.
The fake hyperbolicity given by η is clearly shown in **D** and **E**, where a parabolic SM S_0 and an elliptic one $S_{-1/20}$ are presented: in the first case the maximum spreading grows linearly, whereas in the second one it remains confined, and the estimate given by the surrounding circles of radii growing as powers of η is inappropriate.
Note that in all examples **C**–**E**, the black circles of radii $\eta\, \boldsymbol{v}$ rightly surround $B^1_{\boldsymbol{v}}$.

Theorem 2 (Dynamical localization with $\{|C_{\mathcal{N}}(\boldsymbol{x})\rangle\}$ states)

For $\alpha \in \mathbb{R}$, $\beta \in \mathbb{R}^+ \setminus (0, 2\,]$ and $d_0 > 0$, there exists $N_0 = N_0(\alpha, \beta, d_0) \in \mathbb{N}^+$ with the following property: if $N > N_0$ and $n < \frac{1}{\beta} \frac{\log N}{\log \eta}$, then

$$d_{\mathbb{T}^2}\left(S^n_\alpha\left(\boldsymbol{x}\right), \boldsymbol{y}\right) \geqslant d_0 \Longrightarrow \left\langle C_{\mathcal{N}}(\boldsymbol{x}) \,\middle|\, W^n_{\alpha,N}\, C_{\mathcal{N}}(\boldsymbol{y}) \right\rangle = 0\ ,$$

for all $\boldsymbol{y} \in \mathbb{T}^2$ and $\boldsymbol{x} \in G^N_n\left(\frac{\widetilde{N}}{2N}\right)$, where $W^n_{\alpha,N}$ is the unitary operator defined *in* (14), $\widetilde{N} = 2\sqrt{2}\left(\sqrt{2}+1\right)\eta^{2n}$ *and* $G_n^N(\varepsilon)$ *has been introduced in Definitions 5.1.*

In order to prove Theorem 2, we need the following result, whose proof can be found in Appendix B.

Proposition 5.1

With the notation of Definitions 3.1 and 5.1, and with $[E]^\circ$ denoting the complement of $E \subseteq \mathbb{T}^2$, $[E]^\circ := \mathbb{T}^2 \setminus E$, the following inclusions hold:

$$\left[\overline{\Gamma}_n\left(\varepsilon + \frac{1}{\sqrt{2}N}\right)\right]^\circ \subseteq G_n^N(\varepsilon) \subseteq \left[\overline{\Gamma}_n\left(\varepsilon - \frac{1}{\sqrt{2}N}\right)\right]^\circ \cdot \tag{22}$$

Further, for $\alpha \in \mathbb{R}$ and $n \in \mathbb{N}^+$, if

$$N > \widetilde{N} = 2\sqrt{2}\left(\sqrt{2}+1\right)\eta^{2n} \quad \text{and} \quad \boldsymbol{x} \in G_n^N\left(\frac{\widetilde{N}}{2N}\right) \quad \text{then}$$

$$d_{\mathbb{T}^2}\left(\frac{U_\alpha^p(N\boldsymbol{x})}{N}, \frac{V_\alpha^p(\hat{\boldsymbol{x}}_N)}{N}\right) \leqslant \frac{\sqrt{2}}{N}\left(\frac{\eta^{p+1}-1}{\eta-1}\right) \quad , \quad \forall p \leqslant n \cdot \tag{23}$$

Proof of Theorem 2 :

Using the definition of $\{|C_{\mathcal{N}}(\boldsymbol{x})\rangle\}$ in (6), we easily compute

$$\left\langle C_{\mathcal{N}}(\boldsymbol{x}) \,\middle|\, W_{\alpha,N}^n\, C_{\mathcal{N}}(\boldsymbol{y})\right\rangle = \left\langle \hat{\boldsymbol{x}}_N \,\middle|\, V_\alpha^{-n}(\hat{\boldsymbol{y}}_N)\right\rangle = \delta^{(N)}_{V_\alpha^n(\hat{\boldsymbol{x}}_N)\,,\,\hat{\boldsymbol{y}}_N} \cdot \tag{24}$$

Using the triangular inequality, we get:

$$d_{\mathbb{T}^2}\left(\frac{U_\alpha^n(N\boldsymbol{x})}{N}, \boldsymbol{y}\right) \leqslant d_{\mathbb{T}^2}\left(\frac{U_\alpha^n(N\boldsymbol{x})}{N}, \frac{V_\alpha^n(\hat{\boldsymbol{x}}_N)}{N}\right) + \\ + d_{\mathbb{T}^2}\left(\frac{V_\alpha^n(\hat{\boldsymbol{x}}_N)}{N}, \frac{\hat{\boldsymbol{y}}_N}{N}\right) + d_{\mathbb{T}^2}\left(\frac{\hat{\boldsymbol{y}}_N}{N}, \boldsymbol{y}\right)$$

or equivalently, using the Definitions (10),

$$d_{\mathbb{T}^2}\left(\frac{V_\alpha^n(\hat{\boldsymbol{x}}_N)}{N}, \frac{\hat{\boldsymbol{y}}_N}{N}\right) \geqslant d_{\mathbb{T}^2}\left(S_\alpha^n(\boldsymbol{x}), \boldsymbol{y}\right) - \\ - d_{\mathbb{T}^2}\left(\frac{U_\alpha^n(N\boldsymbol{x})}{N}, \frac{V_\alpha^n(\hat{\boldsymbol{x}}_N)}{N}\right) - d_{\mathbb{T}^2}\left(\frac{\hat{\boldsymbol{y}}_N}{N}, \boldsymbol{y}\right) \cdot$$

Now, since $d_{\mathbb{T}^2}\left(S_\alpha^n(\boldsymbol{x})\,,\,\boldsymbol{y}\right)\geqslant d_0$ by hypothesis, using (40) in Appendix B and observing that $\boldsymbol{x}\in G_n^N\left(\frac{\widetilde{N}}{2N}\right)$ permits us to use (23) in Proposition 5.1, namely that

$$N>\widetilde{N}\implies d_{\mathbb{T}^2}\left(\frac{U_\alpha^n(N\boldsymbol{x})}{N},\frac{V_\alpha^n(\hat{\boldsymbol{x}}_N)}{N}\right)\leqslant\frac{\sqrt{2}}{N}\left(\frac{\eta^{n+1}-1}{\eta-1}\right)\;, \tag{25}$$

we can derive

$$d_{\mathbb{T}^2}\left(\frac{V_\alpha^n(\hat{\boldsymbol{x}}_N)}{N}\,,\,\frac{\hat{\boldsymbol{y}}_N}{N}\right)\geqslant d_0-\frac{\sqrt{2}}{N}\left(\frac{\eta^{n+1}-1}{\eta-1}\right)-\frac{1}{\sqrt{2}N}\;\cdot$$

The r.h.s. of the previous inequality can always be made strictly larger than $\frac{1}{N}$,

$$d_{\mathbb{T}^2}\left(\frac{V_\alpha^n(\hat{\boldsymbol{x}}_N)}{N}\,,\,\frac{\hat{\boldsymbol{y}}_N}{N}\right)>\frac{1}{N}\;, \tag{26}$$

by choosing an N larger than

$$N_{\mathsf{M}}(n)=\max\left\{\frac{1}{d_0}\left[1+\sqrt{2}\left(\frac{\eta^{n+1}-1}{\eta-1}\right)+\frac{1}{\sqrt{2}}\right]\;,\;\widetilde{N}=2\sqrt{2}\left(\sqrt{2}+1\right)\eta^{2n}\right\}\;, \tag{27}$$

so that the condition on the l.h.s. of (25) is also satisfied. From (24) and (26), we have

$$N>N_{\mathsf{M}}(n)\quad\implies\quad\left\langle C_{\mathcal{N}}(\boldsymbol{x})\,\middle|\,W_{\alpha,N}^n\,C_{\mathcal{N}}(\boldsymbol{y})\right\rangle=0\;\cdot \tag{28}$$

Indeed, if the toral distance between two points $(\boldsymbol{z},\boldsymbol{w})$ exceeds $\frac{1}{N}$, then the corresponding grid points $(\hat{\boldsymbol{z}}_N,\hat{\boldsymbol{w}}_N)$ are different and then the periodic Kronecker delta in (24) vanishes. Since the (non–decreasing) function N_{M} in (27) is eventually bounded by $\eta^{\beta n}$ (β being strictly greater than two), we define $\overline{n}$ as the time when $N_{\mathsf{M}}(\overline{n})=\eta^{\beta\overline{n}}=:N_0$, and choose $N>N_0$, $\boldsymbol{x}\in G_n^N\left(\frac{\widetilde{N}}{2N}\right)$. Thus, if $0<n<\overline{n}$, then $N>N_0=N_{\mathsf{M}}(\overline{n})>N_{\mathsf{M}}(n)$, whereas if $\overline{n}\leqslant n<\frac{1}{\beta}\frac{\log N}{\log\eta}$, then $N>\eta^{\beta n}>N_{\mathsf{M}}(n)$ and (28) holds for all $0<n<\frac{1}{\beta}\frac{\log N}{\log\eta}$. ■

In order to proceed with the proof of Theorem 1, we need another auxiliary result which is proved in Appendix C.

Proposition 5.2

With the notation of Definition 5.1, the following relations hold for all $p\in\mathbb{N}$, $n\in\mathbb{N}^+$ and $\varepsilon\in\mathbb{R}^+$:

$$l(\gamma_p)\leqslant\eta^p\;, \tag{29a}$$

$$\mu\left(\overline{\gamma}_p(\varepsilon)\right)\leqslant 2\,\varepsilon\,\eta^p+\pi\varepsilon^2\;, \tag{29b}$$

$$\mu\left(\overline{\Gamma}_n\left(\varepsilon\right)\right) \leqslant 2\left(\sqrt{2}+1\right)\varepsilon\,\eta^n + \pi\,n\,\varepsilon^2 \cdot \tag{29c}$$

Moreover, if $N \in \mathbb{N}^+$ and $\widetilde{N} = 2\sqrt{2}\left(\sqrt{2}+1\right)\eta^{2n}$ (cfr. equation (23) in Proposition 5.1):

$$N > \widetilde{N} \Longrightarrow \mu\left(\left[G_n^N\left(\frac{\widetilde{N}}{2N}\right)\right]^{\circ}\right) \leqslant \frac{38\,\eta^{3n}}{N} \cdot \tag{29d}$$

We are finally in position to conclude with

Proof of Theorem 1:

We subdivide the proof in two steps: in the first we concentrate on continuous f, that is $f \in \mathcal{C}^0\left(\mathbb{T}^2\right)\left(\subset L^2_\mu\left(\mathbb{T}^2\right)\right)$; in the second one we extend the result to essentially bounded function by applying the following Corollary of Lusin's Theorem [21, 30, 31]:

> *Given $f \in L^\infty_\mu\left(\mathcal{X}\right)$, with $\mathcal{X}$ compact, there exists a sequence $\{f_n\}$ of continuous functions on $\mathcal{X}$ such that $|f_n| \leq \|f\|_\infty$ and converging to f μ – almost everywhere.*

(1) Let $f \in \mathcal{C}^0\left(\mathbb{T}^2\right)$ and $\mathrm{Op}_{j,N}\left(f\right) := \left(\Theta^j_\alpha - \mathcal{J}_{\infty,\mathcal{N}} \circ \Theta^j_{\mathcal{N},\alpha} \circ \mathcal{J}_{\mathcal{N},\infty}\right)\left(f\right)$: notice that $\mathrm{Op}_{j,N}\left(f\right)$ is a multiplication operator on $L^2_\mu\left(\mathbb{T}^2\right)$, but also an $L^\infty_\mu\left(\mathbb{T}^2\right)$ $\big($and thus also an $L^2_\mu\left(\mathbb{T}^2\right)\big)$ function. According to (21), we must show that

$$\forall g \in L^2_\mu\left(\mathbb{T}^2\right) \quad , \quad \lim_{\substack{j,N\to\infty \\ j<\frac{1}{\gamma}\frac{\log N}{\log \eta}}} \left\|\ \mathrm{Op}_{j,N}\left(f\right)\ g\ \right\|_2 = 0 \quad \cdot$$

Using Schwartz's inequality first with g in the class of *simple functions* and then using their density in $L^2_\mu\left(\mathbb{T}^2\right)$, we have just to show that

$$\lim_{\substack{j,N\to\infty \\ j<\frac{1}{\gamma}\frac{\log N}{\log \eta}}} \left\|\ \mathrm{Op}_{j,N}\left(f\right)\ \right\|_2 = 0 \quad \cdot$$

Explicitly, using (1), we write:

$$\begin{aligned}\left\|\ \mathrm{Op}_{j,N}\left(f\right)\ \right\|_2^2 = \omega_\mu\left(\mathrm{Op}_{j,N}\left(f\right)^*\mathrm{Op}_{j,N}\left(f\right)\right) = \omega_\mu\left[\left(\Theta^j_\alpha f\right)^*\left(\Theta^j_\alpha f\right)\right] + \\ + \omega_\mu\left[\left(\mathcal{J}_{\infty,\mathcal{N}} \circ \Theta^j_{\mathcal{N},\alpha} \circ \mathcal{J}_{\mathcal{N},\infty}\right)\left(f\right)^*\left(\mathcal{J}_{\infty,\mathcal{N}} \circ \Theta^j_{\mathcal{N},\alpha} \circ \mathcal{J}_{\mathcal{N},\infty}\right)\left(f\right)\right] + \\ - 2\,\mathrm{Re}\left\{\omega_\mu\left[\left(\Theta^j_\alpha f\right)^*\left(\mathcal{J}_{\infty,\mathcal{N}} \circ \Theta^j_{\mathcal{N},\alpha} \circ \mathcal{J}_{\mathcal{N},\infty}\right)\left(f\right)\right]\right\} \ ,\end{aligned}$$

which, via Proposition 3.2.1, becomes

$$\begin{aligned}
&= \omega_\mu\left[\Theta^j_\alpha\left(\overline{f}\right)\Theta^j_\alpha\left(f\right)\right] - 2\,\mathrm{Re}\left\{\tau_{\mathcal{N}}\left[\mathcal{J}_{\mathcal{N},\infty}\left(\Theta^j_\alpha f\right)^*\left(\Theta^j_{\mathcal{N},\alpha}\circ\mathcal{J}_{\mathcal{N},\infty}\right)(f)\right]\right\} + \\
&\quad + \tau_{\mathcal{N}}\left[\left(\mathcal{J}_{\mathcal{N},\infty}\circ\mathcal{J}_{\infty,\mathcal{N}}\circ\Theta^j_{\mathcal{N},\alpha}\circ\mathcal{J}_{\mathcal{N},\infty}\right)(f)^*\left(\Theta^j_{\mathcal{N},\alpha}\circ\mathcal{J}_{\mathcal{N},\infty}\right)(f)\right]\ ,
\end{aligned}$$

that, using Proposition 3.2.3, can be recast as

$$\begin{aligned}
&= \left(\omega_\mu\circ\Theta^j_\alpha\right)\left(\overline{f}f\right) + \tau_{\mathcal{N}}\left[\left(\Theta^j_{\mathcal{N},\alpha}\circ\mathcal{J}_{\mathcal{N},\infty}\right)(f)^*\left(\Theta^j_{\mathcal{N},\alpha}\circ\mathcal{J}_{\mathcal{N},\infty}\right)(f)\right] + \\
&\quad - 2\,\mathrm{Re}\left\{\tau_{\mathcal{N}}\left[\left(\mathcal{J}_{\mathcal{N},\infty}\circ\Theta^j_\alpha\right)(f)^*\left(\Theta^j_{\mathcal{N},\alpha}\circ\mathcal{J}_{\mathcal{N},\infty}\right)(f)\right]\right\} \\
&= \omega_\mu\left(|f|^2\right) + \left(\tau_{\mathcal{N}}\circ\Theta^j_{\mathcal{N},\alpha}\right)\left[\mathcal{J}_{\mathcal{N},\infty}(f)^*\,\mathcal{J}_{\mathcal{N},\infty}(f)\right] - 2\,\mathrm{Re}\left(I_{j,N}(f)\right)\ ,
\end{aligned}$$

with

$$\begin{aligned}
I_{j,N}(f) &:= \tau_{\mathcal{N}}\left[\left(\mathcal{J}_{\mathcal{N},\infty}\circ\Theta^j_\alpha\right)(f)^*\left(\Theta^j_{\mathcal{N},\alpha}\circ\mathcal{J}_{\mathcal{N},\infty}\right)(f)\right] \\
&= \mathcal{N}\int_{\mathbb{T}^2}\mu(\mathrm{d}\boldsymbol{x})\int_{\mathbb{T}^2}\mu(\mathrm{d}\boldsymbol{y})\,\overline{f(\boldsymbol{y})}\,f(S^j_\alpha\boldsymbol{x})|\langle C_{\mathcal{N}}(\boldsymbol{x}), W^j_{\alpha,N}C_{\mathcal{N}}(\boldsymbol{y})\rangle|^2\ .
\end{aligned}$$

Now, Proposition 3.2.2 yields

$$\left(\tau_{\mathcal{N}}\circ\Theta^j_{\mathcal{N},\alpha}\right)\left[\mathcal{J}_{\mathcal{N},\infty}(f)^*\,\mathcal{J}_{\mathcal{N},\infty}(f)\right] = \tau_{\mathcal{N}}\left[\mathcal{J}_{\mathcal{N},\infty}(f)^*\,\mathcal{J}_{\mathcal{N},\infty}(f)\right] \xrightarrow[N\longrightarrow\infty]{} \omega_\mu\left(|f|^2\right)\ ,$$

so that the strategy is to prove that also $I_{j,N}(f)$ goes to $\omega_\mu\left(|f|^2\right) = \int_{\mathbb{T}^2}\mu(\mathrm{d}\boldsymbol{x})|f(\boldsymbol{x})|^2$ when $j, N\to\infty$ with $j < \frac{1}{\gamma}\frac{\log N}{\log\eta}$.

Resorting to $G^N_n\left(\frac{\widetilde{N}}{2N}\right)$ in Definition 5.1, and to its complementary set $\left[G^N_n\left(\frac{\widetilde{N}}{2N}\right)\right]^\circ = \mathbb{T}^2\setminus G^N_n\left(\frac{\widetilde{N}}{2N}\right)$, we can write

$$\begin{aligned}
&\left|I_{j,N}(f) - \int_{\mathbb{T}^2}\mu(\mathrm{d}\boldsymbol{y})\,|f(\boldsymbol{y})|^2\right| \\
&= \left|\int_{\mathbb{T}^2}\mu(\mathrm{d}\boldsymbol{x})\int_{\mathbb{T}^2}\mu(\mathrm{d}\boldsymbol{y})\,\overline{f(\boldsymbol{y})}\left(f(S^j_\alpha\boldsymbol{x}) - f(\boldsymbol{y})\right)\mathcal{N}|\langle C_{\mathcal{N}}(\boldsymbol{x}), W^j_{\alpha,N}C_{\mathcal{N}}(\boldsymbol{y})\rangle|^2\right| \\
&\leq \left|\int_{\left[G^N_n\left(\frac{\widetilde{N}}{2N}\right)\right]^\circ}\mu(\mathrm{d}\boldsymbol{x})\int_{\mathbb{T}^2}\mu(\mathrm{d}\boldsymbol{y})\,\overline{f(\boldsymbol{y})}\left(f(S^j_\alpha\boldsymbol{x}) - f(\boldsymbol{y})\right)\mathcal{N}|\langle C_{\mathcal{N}}(\boldsymbol{x}), W^j_{\alpha,N}C_{\mathcal{N}}(\boldsymbol{y})\rangle|^2\right| \\
&+ \left|\int_{G^N_n\left(\frac{\widetilde{N}}{2N}\right)}\mu(\mathrm{d}\boldsymbol{x})\int_{\mathbb{T}^2}\mu(\mathrm{d}\boldsymbol{y})\overline{f(\boldsymbol{y})}\left(f(S^j_\alpha\boldsymbol{x}) - f(\boldsymbol{y})\right)\mathcal{N}|\langle C_{\mathcal{N}}(\boldsymbol{x}), W^j_{\alpha,N}C_{\mathcal{N}}(\boldsymbol{y})\rangle|^2\right|. \qquad (30)
\end{aligned}$$

For the first integral in the r.h.s. of the previous expression we have:

$$
\begin{aligned}
&\left|\int_{\left[G_n^N\left(\frac{\widetilde{N}}{2N}\right)\right]^\circ}\mu(\mathrm{d}\boldsymbol{x})\int_{\mathbb{T}^2}\mu(\mathrm{d}\boldsymbol{y})\,\overline{f(\boldsymbol{y})}\big(f(S_\alpha^j\boldsymbol{x})-f(\boldsymbol{y})\big)\mathcal{N}|\langle C_{\mathcal{N}}(\boldsymbol{x}),W_{\alpha,N}^jC_{\mathcal{N}}(\boldsymbol{y})\rangle|^2\right|\\
&\leq 2(\|f\|_\infty)^2\int_{\left[G_n^N\left(\frac{\widetilde{N}}{2N}\right)\right]^\circ}\mu(\mathrm{d}\boldsymbol{x})\int_{\mathbb{T}^2}\mu(\mathrm{d}\boldsymbol{y})\,\mathcal{N}|\langle\big(W_{\alpha,N}^*\big)^jC_{\mathcal{N}}(\boldsymbol{x}),C_{\mathcal{N}}(\boldsymbol{y})\rangle|^2\\
&\leq 2(\|f\|_\infty)^2\mu\left(\left[G_n^N\left(\frac{\widetilde{N}}{2N}\right)\right]^\circ\right)\leqslant\frac{76\,\eta^{3j}}{N}(\|f\|_\infty)^2
\end{aligned}
$$

where we have used completeness and normalization Properties 3.1 and equation (29d) from Proposition 5.2; this term becomes negligible for large $N>\widetilde{N}$ iff $j<\frac{1}{\gamma}\frac{\log N}{\log\eta}$, with $\gamma>3$.

Now it remains to prove that the second term in (30) is also negligible for large N: selecting a ball $B(S_\alpha^j\boldsymbol{x},d_0)$, one derives

$$
\begin{aligned}
&\left|\int_{G_n^N\left(\frac{\widetilde{N}}{2N}\right)}\mu(\mathrm{d}\boldsymbol{x})\int_{\mathbb{T}^2}\mu(\mathrm{d}\boldsymbol{y})\,\overline{f(\boldsymbol{y})}\,\big(f(S_\alpha^j\boldsymbol{x})-f(\boldsymbol{y})\big)\,\mathcal{N}|\langle C_{\mathcal{N}}(\boldsymbol{x}),W_{\alpha,N}^jC_{\mathcal{N}}(\boldsymbol{y})\rangle|^2\right|\\
&\leq\left|\int_{G_n^N\left(\frac{\widetilde{N}}{2N}\right)}\mu(\mathrm{d}\boldsymbol{x})\int_{B(S_\alpha^j\boldsymbol{x},d_0)}\mu(\mathrm{d}\boldsymbol{y})\,\overline{f(\boldsymbol{y})}\big(f(S_\alpha^j\boldsymbol{x})-f(\boldsymbol{y})\big)\mathcal{N}|\langle C_{\mathcal{N}}(\boldsymbol{x}),W_{\alpha,N}^jC_{\mathcal{N}}(\boldsymbol{y})\rangle|^2\right|\\
&+\left|\int_{G_n^N\left(\frac{\widetilde{N}}{2N}\right)}\mu(\mathrm{d}\boldsymbol{x})\int_{\mathbb{T}^2\setminus B(S_\alpha^j\boldsymbol{x},d_0)}\mu(\mathrm{d}\boldsymbol{y})\overline{f(\boldsymbol{y})}\big(f(S_\alpha^j\boldsymbol{x})-f(\boldsymbol{y})\big)\mathcal{N}|\langle C_{\mathcal{N}}(\boldsymbol{x}),W_{\alpha,N}^jC_{\mathcal{N}}(\boldsymbol{y})\rangle|^2\right|.
\end{aligned}
$$

Applying the mean value theorem in the first double integral, we get that $\exists\boldsymbol{c}\in B(S_\alpha^j\boldsymbol{x},d_0)$ such that

$$
\begin{aligned}
&\left|\int_{G_n^N\left(\frac{\widetilde{N}}{2N}\right)}\mu(\mathrm{d}\boldsymbol{x})\int_{\mathbb{T}^2}\mu(\mathrm{d}\boldsymbol{y})\,\overline{f(\boldsymbol{y})}\,\big(f(S_\alpha^j\boldsymbol{x})-f(\boldsymbol{y})\big)\,\mathcal{N}|\langle C_{\mathcal{N}}(\boldsymbol{x}),W_{\alpha,N}^jC_{\mathcal{N}}(\boldsymbol{y})\rangle|^2\right|\\
&\leq\int_{G_n^N\left(\frac{\widetilde{N}}{2N}\right)}\mu(\mathrm{d}\boldsymbol{x})\,\left|\overline{f(\boldsymbol{c})}\,\big(f(S_\alpha^j\boldsymbol{x})-f(\boldsymbol{c})\big)\right|\int_{B(S_\alpha^j\boldsymbol{x},d_0)}\mu(\mathrm{d}\boldsymbol{y})\,\mathcal{N}|\langle\big(W_{\alpha,N}^*\big)^jC_{\mathcal{N}}(\boldsymbol{x}),C_{\mathcal{N}}(\boldsymbol{y})\rangle|^2\\
&\quad+2\|f\|_\infty^2\int_{G_n^N\left(\frac{\widetilde{N}}{2N}\right)}\mu(\mathrm{d}\boldsymbol{x})\int_{\mathbb{T}^2\setminus B(S_\alpha^j\boldsymbol{x},d_0)}\mu(\mathrm{d}\boldsymbol{y})\mathcal{N}|\langle C_{\mathcal{N}}(\boldsymbol{x}),W_{\alpha,N}^jC_{\mathcal{N}}(\boldsymbol{y})\rangle|^2\ .
\end{aligned}
$$

Finally, using completeness and normalization (Properties 3.1), we arrive at the upper bound

$$\leq \|f\|_\infty \sup_{\substack{\boldsymbol{z}\in\mathbb{T}^2\\ \boldsymbol{c}\in B(\boldsymbol{z},d_0)}} \left|\left(f(\boldsymbol{z})-f(\boldsymbol{c})\right)\right| + 2\,\|f\|_\infty^2 \quad \mathcal{N} \sup_{\substack{\boldsymbol{x}\in G_n^N\left(\frac{\tilde{N}}{2N}\right)\\ \boldsymbol{y}\notin B(S_\alpha^j\boldsymbol{x},d_0)}} |\langle C_\mathcal{N}(\boldsymbol{x}), W_{\alpha,N}^j C_\mathcal{N}(\boldsymbol{y})\rangle|^2 \cdot$$

By uniform continuity, the first term can be made arbitrarily small, provided we choose d_0 small enough. For the second integral, we use Theorem 2, which provides us with $N_0 = N_0(d_0)$ depending on the same d_0 , such that the second term vanishes for all $N > N_0$ and far all $j < \frac{1}{\gamma}\frac{\log N}{\log \eta}$.

(2) In order to extend the result of point **(1)** to $f \in L^\infty_\mu\left(\mathbb{T}^2\right)$, we use the Corollary of Lusin's Theorem, choose a sequence $\{f_n\}_n$ as in its statement and estimate

$$\lim_{\substack{j,N\to\infty\\ j<\frac{1}{\gamma}\frac{\log N}{\log\eta}}} \left\| \operatorname{Op}_{j,N}(f) \right\|_2 \leqslant \lim_{\substack{j,N\to\infty\\ j<\frac{1}{\gamma}\frac{\log N}{\log\eta}}} \left\| \operatorname{Op}_{j,N}(f-f_n) \right\|_2 + \lim_{\substack{j,N\to\infty\\ j<\frac{1}{\gamma}\frac{\log N}{\log\eta}}} \left\| \operatorname{Op}_{j,N}(f_n) \right\|_2 \cdot$$

Using point **(1)**, the second term in the r.h.s. of the previous equation can be bounded by arbitrarily small ε, indeed $f_n \in \mathcal{C}^0\left(\mathbb{T}^2\right)$.

For the first term we proceed as follows: using Definition 4.1 together with equations (37) and (38) of Appendix A, we find

$$\left(\mathcal{J}_{\infty,\mathcal{N}} \circ \Theta^j_{\mathcal{N},\alpha} \circ \mathcal{J}_{\mathcal{N},\infty}\right)(g)(\boldsymbol{x}) = \sum_{\boldsymbol{\ell}\in(\mathbb{Z}/N\mathbb{Z})^2} \Gamma_N(g)\left(\frac{V_\alpha(\boldsymbol{\ell})}{N}\right)\ \mathcal{X}_{Q_N\left(\frac{\boldsymbol{\ell}}{N}\right)}(\boldsymbol{x})\ , \qquad (31)$$

where g is any measurable function on $\mathbb{T}^2$. Then, because of how the running average operator (RAO) Γ_N is defined, for all $g \in L^1_\mu\left(\mathbb{T}^2\right)$ it follows that

$$\left\|\left(\mathcal{J}_{\infty,\mathcal{N}} \circ \Theta^j_{\mathcal{N},\alpha} \circ \mathcal{J}_{\mathcal{N},\infty}\right)(g)\right\|_1 \leqslant \left\|\left(\mathcal{J}_{\infty,\mathcal{N}} \circ \Theta^j_{\mathcal{N},\alpha} \circ \mathcal{J}_{\mathcal{N},\infty}\right)(|g|)\right\|_1 = \|g\|_1\ ,$$

where $\|\cdot\|_1$ denotes the $L^1_\mu\left(\mathbb{T}^2\right)$–norm, and that

$$\left\|\left(\mathcal{J}_{\infty,\mathcal{N}} \circ \Theta^j_{\mathcal{N},\alpha} \circ \mathcal{J}_{\mathcal{N},\infty}\right)(g)\right\|_\infty = \sup_{\boldsymbol{\ell}\in(\mathbb{Z}/N\mathbb{Z})^2} \left\{\left|\Gamma_N(g)\left(\frac{\boldsymbol{\ell}}{N}\right)\right|\right\} \leqslant \|\Gamma_N(g)\|_0 \leqslant \|g\|_\infty \cdot$$

Indeed, the first equality in the last formula comes from the definition of essential norm [21] (which in this case amounts to the greater absolute value assumed by the simple function $\mathcal{J}_{\infty,\mathcal{N}} \circ \Theta^j_{\mathcal{N},\alpha} \circ \mathcal{J}_{\mathcal{N},\infty}$), whereas the first inequality is a consequence of the continuity of Γ_N and the last one from Proposition A.1. Putting last two inequality together, we obtain

$$\left\| \left(\mathcal{J}_{\infty,\mathcal{N}} \circ \Theta^{j}_{\mathcal{N},\alpha} \circ \mathcal{J}_{\mathcal{N},\infty} \right)(g) \right\|_2 \leqslant \|g\|_\infty \|g\|_1 \ ,$$

whence, setting $g = f - f_n$,

$$\begin{aligned} \| \ \mathrm{Op}_{j,N}\,(f - f_n) \ \|_2 &= \left\| \ \Theta^{j}_{\alpha}\,(f - f_n) - \mathcal{J}_{\infty,\mathcal{N}} \circ \Theta^{j}_{\mathcal{N},\alpha} \circ \mathcal{J}_{\mathcal{N},\infty}\,(f - f_n) \ \right\|_2 \\ &\leqslant \| \ f - f_n \ \|_2 + \| \ f - f_n \ \|_\infty \| \ f - f_n \ \|_1 \quad , \quad \forall j, N \ \cdot \end{aligned} \tag{32}$$

Now convergence follows from Lusin's Corollary. ■

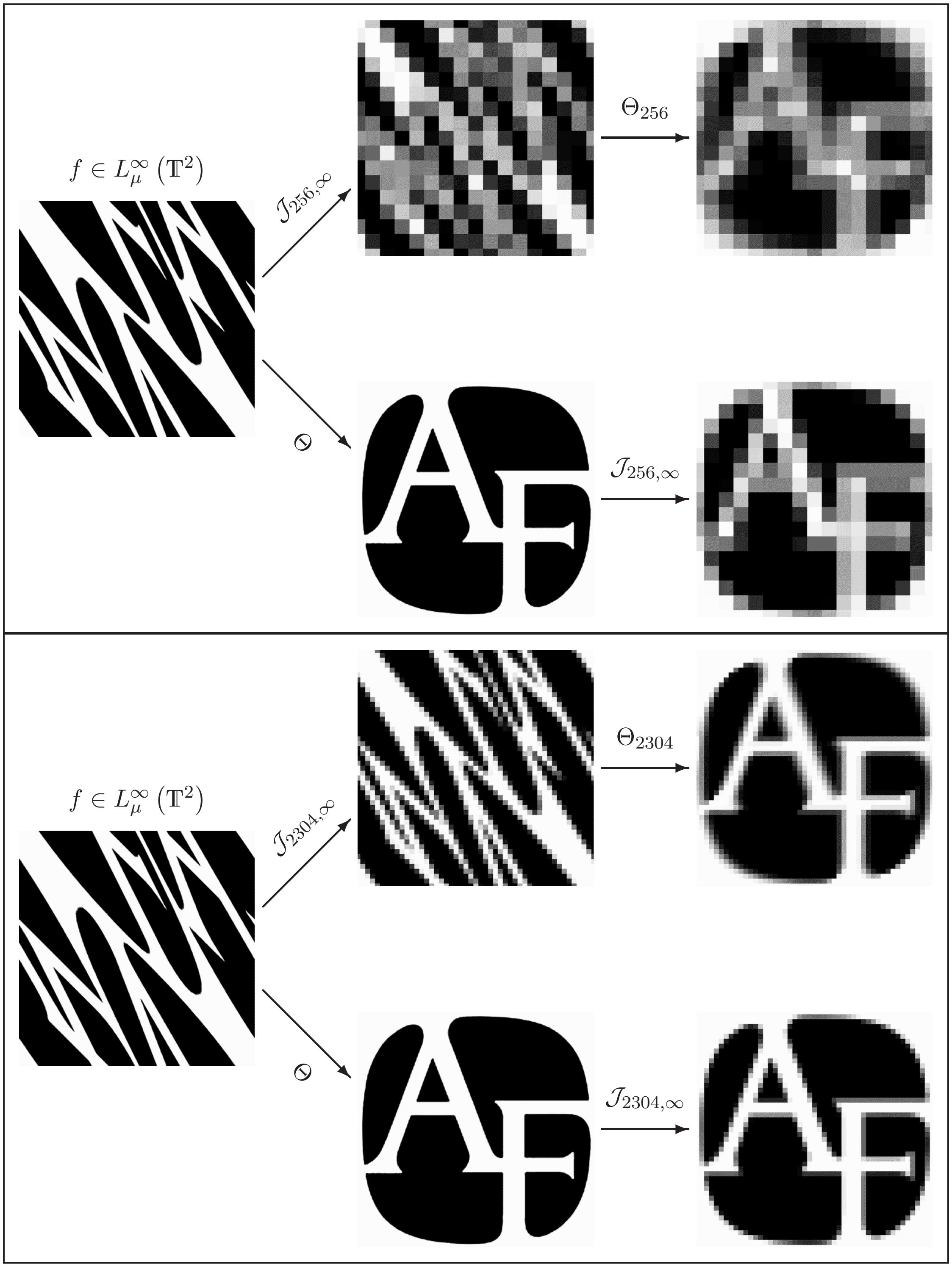

Figure 4: These two plots show how the difference between $\mathcal{J}_{\mathcal{N},\infty} \circ \Theta_\alpha$ and $\Theta_{\mathcal{N},\alpha} \circ \mathcal{J}_{\mathcal{N},\infty}$ becomes smaller with N. For the continuous SM, Θ_1, the actions $\mathcal{J}_{\mathcal{N},\infty} \circ \Theta_1$ and $\Theta_{\mathcal{N},1} \circ \mathcal{J}_{\mathcal{N},\infty}$ on $f \in L^\infty_\mu(\mathbb{T}^2)$ (left part of both plots) are plotted for two different N: $N = 16$ (top) and $N = 48$ (bottom). The resulting matrices are mapped back, together with the function $\Theta_1(f)$, on the unfolded torus, by means of the de–discretization operator $\mathcal{J}_{\infty,\mathcal{N}}$.

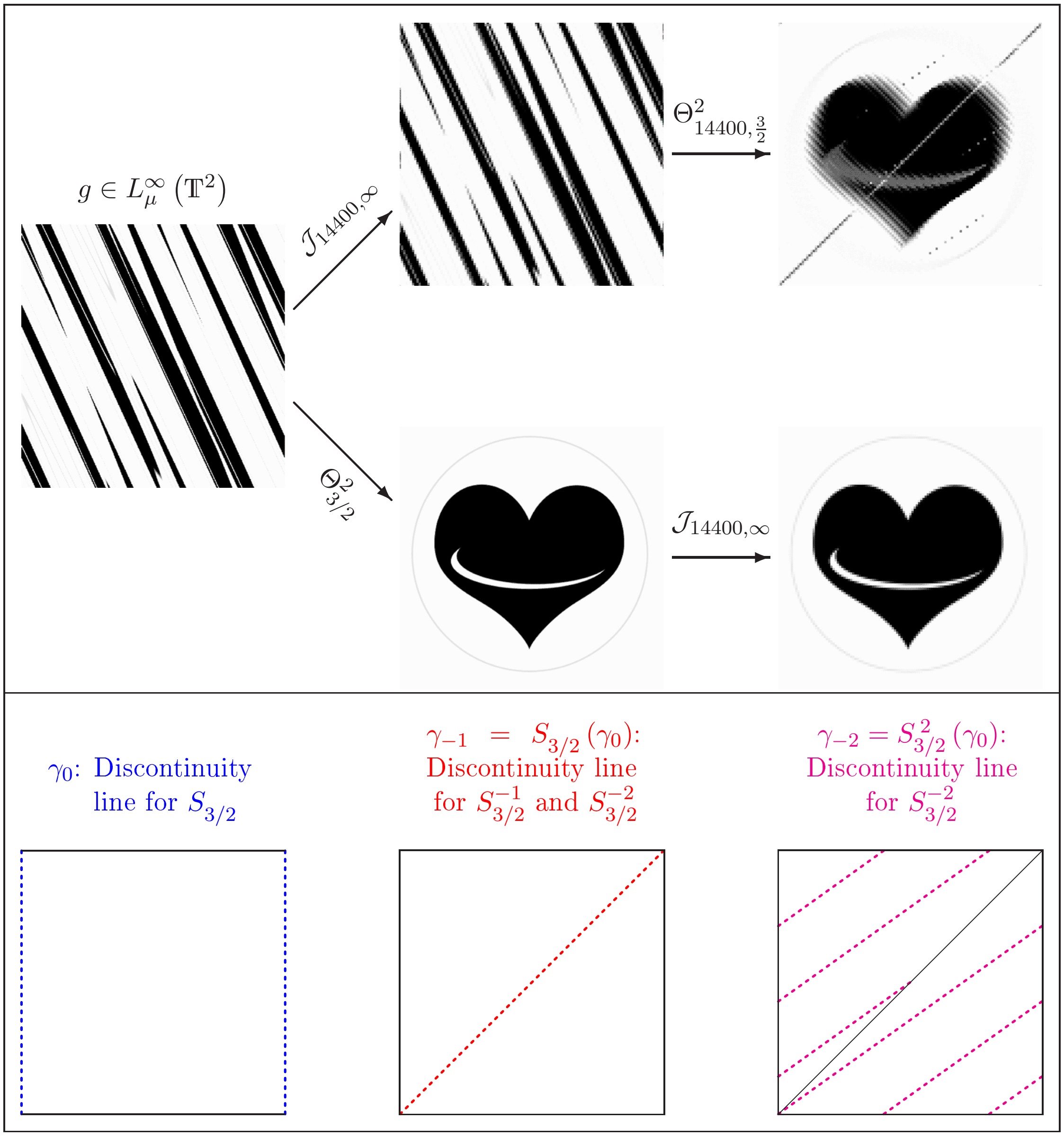

Figure 5: Here, the same picture as in Figure 4, is represented, with a finer discretization given by $N = 120$ and a different function $g \in L^\infty_\mu\left(\mathbb{T}^2\right)$, for a discontinuous SM, $\Theta_{3/2}$, acting two times. Choosing a function g with sharp variation across γ_0 (blue lines), the preimage of γ_{-1}, the discontinuity of $\Theta_{3/2}$ makes it evident how the differences between $\mathcal{J}_{14400,\infty} \circ \Theta^2_\alpha$ and $\Theta^2_{14400,\alpha} \circ \mathcal{J}_{14400,\infty}$ are the greater the closer they are to the discontinuity line γ_{-1} (red lines). Of course, the longer the temporal evolution, the worst the correspondence, in the sense that several new discontinuity lines come to play a role. In the case at hands, the map acts twice, and γ_{-2} is felt by $\Theta^2_{14400,\alpha} \circ \mathcal{J}_{14400,\infty}$, as expected.

6. Conclusions

In this article we have considered discrete approximants of Sawtooth Maps on the torus and we have studied them in an algebraic framework modeled on the so–called Anti–Wick quantization; In fact, finite–dimensional discretization and quantization can be seen as similar procedures in that they map an abelian Von Neumann algebra (of essentially bounded functions on phase–space) into finite–dimensional matrix subalgebras, the only difference being whether the latter are diagonal (commutative) or not.

In the semi–classical analysis of classically chaotic quantum systems, the correspondence classical/quantum is usually observed only on time–scales that are logarithmic in the quantization parameter $\hbar$. The motivation of our study was to show that the same phenomenon arises when a hyperbolic classical system is discretized, namely forced to move on a lattice, and afterwards the lattice spacing is sent to zero.

Previous results [14] based on the numerical investigation of the entropy production, indicate that it should indeed be so; however, these results were not supported by a solid framework where to analyze the continuous limit of the family of discrete approximants. This is the content of this article.

The major difficulty was represented by the need of controlling the discontinuous character of Sawtooth Maps, which was made possible by an appropriate choice of Lattice States. In fact, similarly to the entropic approach which, despite the dynamics being classical, was based on a quantum dynamical entropy, the discretization/de–discretization procedure we set up is based on quantum tools.

The choice of Lattice States was naturally pointed to by the lattice structure of the discrete phase–space and turned out to posses the right localization properties for mastering the discontinuities. The result is the appearance of a logarithmic time–scale when the discrete hyperbolic SM tend to their continuous limit; namely, the continuous and discrete dynamics agree up to a *breaking time* which is proportional to the logarithm of the lattice spacing.

The proportionality constant does not involve the Lyapunov exponent, that is the eigenvalue $\lambda > 1$ of the dynamical matrix S_α, rather the largest eigenvalue, η, of $\sqrt{S_\alpha^\dagger S_\alpha}$. In the case of elliptic SM, $|\lambda| = 1$, $\eta > \sqrt{2}$; however the resulting breaking time is a spurious effect, while when $\lambda > 1$, the presence of η in the breaking time seems to be an unavoidable consequence of the discontinuous dynamics.

A. Anti Wick discretization of $L^\infty_\mu\left(\mathbb{T}^2\right)$

In this appendix we will apply Definitions 3.3 and discretize $L^\infty_\mu\left(\mathbb{T}^2\right)$ by means of the LS set $\{|C_\mathcal{N}(\boldsymbol{x})\rangle \mid \boldsymbol{x}\in\mathbb{T}^2\}\in\mathcal{H}_\mathcal{N}$ introduced in Section 3.1.

In this framework, the discretizing/de–discretizing operators of Definitions 3.3 read:

$$L^\infty_\mu\left(\mathbb{T}^2\right)\ni f\mapsto N^2\int_{\mathbb{T}^2}\mu(\mathrm{d}\boldsymbol{x})\,f(\boldsymbol{x})\,|\,\hat{\boldsymbol{x}}_N\,\rangle\langle\,\hat{\boldsymbol{x}}_N\,| =: \mathcal{J}_{\mathcal{N},\infty}(f)\in\mathcal{D}_\mathcal{N}\ , \tag{33}$$

$$\mathcal{D}_\mathcal{N}\ni\mathcal{X}\mapsto\langle\,\hat{\boldsymbol{x}}_N\,|\,X\,|\,\hat{\boldsymbol{x}}_N\,\rangle =: \mathcal{J}_{\infty,\mathcal{N}}(X)(\boldsymbol{x})\in\mathcal{S}\left(\mathbb{T}^2\right)\subset L^\infty_\mu\left(\mathbb{T}^2\right)\ , \tag{34}$$

where $\mathcal{S}\left(\mathbb{T}^2\right)$ denotes the set of *simple functions* [21] on the torus. The matrix elements of $\mathcal{J}_{\mathcal{N},\infty}(f)$ are as follows:

$$\begin{aligned}
M^{(f)}_{\boldsymbol{\ell},\boldsymbol{m}} &:= \langle\,\boldsymbol{\ell}\mid\mathcal{J}_{\mathcal{N},\infty}(f)\mid\boldsymbol{m}\,\rangle\\
&= N^2\int_{\mathbb{T}^2}\mu(\mathrm{d}\boldsymbol{x})\ f(\boldsymbol{x})\ \langle\,\boldsymbol{\ell}\,|\,\hat{\boldsymbol{x}}_N\,\rangle\langle\,\hat{\boldsymbol{x}}_N\,|\,\boldsymbol{m}\,\rangle\\
&= N^2\int_0^1\mathrm{d}x_1\int_0^1\mathrm{d}x_2\ f(\boldsymbol{x})\ \delta^{(N)}_{\ell_1\,,\,\hat{x}_{N,1}}\ \delta^{(N)}_{\ell_2\,,\,\hat{x}_{N,2}}\ \delta^{(N)}_{m_1\,,\,\hat{x}_{N,1}}\ \delta^{(N)}_{m_2\,,\,\hat{x}_{N,2}}\\
&= N^2\ \delta^{(N)}_{\ell_1\,,\,m_1}\ \delta^{(N)}_{\ell_2\,,\,m_2}\int_0^1\mathrm{d}x_1\int_0^1\mathrm{d}x_2\ f(\boldsymbol{x})\ \delta^{(N)}_{\ell_1\,,\,\lfloor Nx_1+\frac{1}{2}\rfloor}\ \delta^{(N)}_{\ell_2\,,\,\lfloor Nx_2+\frac{1}{2}\rfloor}\ .
\end{aligned}$$

This implies

$$M^{(f)}_{\boldsymbol{\ell},\boldsymbol{m}} = N^2\ \delta^{(N)}_{\boldsymbol{\ell},\boldsymbol{m}}\int_{\frac{\ell_1-\frac{1}{2}}{N}}^{\frac{\ell_1+\frac{1}{2}}{N}}\mathrm{d}x_1\int_{\frac{\ell_2-\frac{1}{2}}{N}}^{\frac{\ell_2+\frac{1}{2}}{N}}\mathrm{d}x_2\ f(\boldsymbol{x})\ \ , \tag{35}$$

so that varying $f\in L^\infty_\mu\left(\mathbb{T}^2\right)$ yields $\mathrm{Ran}\left(\mathcal{J}_{\mathcal{N},\infty}\right)=\mathcal{D}_\mathcal{N}$. In order to recast (35) into a nicer expression, we introduce

Definition A.1 (Running Average Operator (RAO))

Let $Q_N\left(\boldsymbol{x}\right)$ denote the square of side $1/N$, oriented parallel to the axis of the torus and centered around $\boldsymbol{x}$; then, the Running Average Operator $\Gamma_N : L^\infty_\mu\left(\mathcal{X}\right)\longmapsto\mathcal{C}^0\left(\mathbb{T}^2\right)$, is defined by

$$L^\infty_\mu\left(\mathbb{T}^2\right)\ni f(\boldsymbol{x})\longmapsto\Gamma_N\left(f\right)\left(\boldsymbol{x}\right) =: N^2\int_{Q_N(\boldsymbol{x})}\mu(\mathrm{d}\boldsymbol{y})\ f(\boldsymbol{y})\ \in\mathcal{C}^0\left(\mathbb{T}^2\right)\ .$$

Proposition A.1

Given $f \in L^\infty_\mu\left(\mathbb{T}^2\right)$, the function $f^{(Q)}_N := \Gamma_N\left(f\right)$ is uniformly continuous on $\mathbb{T}^2$; moreover, the Running Average Operator has norm

$$\|\Gamma_N\|_{\mathcal{B}} := \sup_{f \in L^\infty_\mu(\mathbb{T}^2)} \frac{\|\Gamma_N\left(f\right)\|_0}{\|f\|_\infty} = 1 \cdot \tag{36}$$

Proof:

Let $\boldsymbol{x}_0 \in \mathbb{T}^2$, $\boldsymbol{x} \in Q_N\left(\boldsymbol{x}_0\right)$ and $\mathcal{X}_E$ denote the characteristic function of $E \subset \mathbb{T}^2$. By Definition (A.1):

$$\begin{aligned}
\left| f^{(Q)}_N\left(\boldsymbol{x}_0\right) - f^{(Q)}_N\left(\boldsymbol{x}\right)\right| &= N^2 \left| \int_{\mathbb{T}^2} \mu(\mathrm{d}\boldsymbol{y})\ f(\boldsymbol{y})\ \left(\mathcal{X}_{Q_N(\boldsymbol{x}_0)}(\boldsymbol{y}) - \mathcal{X}_{Q_N(\boldsymbol{x})}(\boldsymbol{y})\right)\right| \\
&\leqslant N^2\ \|f\|_\infty \int_{\mathbb{T}^2} \mu(\mathrm{d}\boldsymbol{y})\ \left|\mathcal{X}_{Q_N(\boldsymbol{x}_0)}(\boldsymbol{y}) - \mathcal{X}_{Q_N(\boldsymbol{x})}(\boldsymbol{y})\right| \\
&= N^2\ \|f\|_\infty \left[\mu\Big(Q_N\left(\boldsymbol{x}_0\right) \cup Q_N\left(\boldsymbol{x}\right)\Big)\ -\ \mu\Big(Q_N\left(\boldsymbol{x}_0\right) \cap Q_N\left(\boldsymbol{x}\right)\Big)\right] \cdot
\end{aligned}$$

According to our hypothesis, $\boldsymbol{x} \in Q_N\left(\boldsymbol{x}_0\right)$, thus geometrical considerations lead to:

$$\begin{aligned}
\mu\Big(Q_N\left(\boldsymbol{x}_0\right) \cup Q_N\left(\boldsymbol{x}\right)\Big) &\leqslant \left(\frac{1}{N} + |x_1 - x_{01}|\right)\left(\frac{1}{N} + |x_2 - x_{02}|\right) \\
\mu\Big(Q_N\left(\boldsymbol{x}_0\right) \cap Q_N\left(\boldsymbol{x}\right)\Big) &= \left(\frac{1}{N} - |x_1 - x_{01}|\right)\left(\frac{1}{N} - |x_2 - x_{02}|\right) \\
\mu\Big(Q_N\left(\boldsymbol{x}_0\right) \cup Q_N\left(\boldsymbol{x}\right)\Big)\ -\ \mu\Big(Q_N\left(\boldsymbol{x}_0\right) \cap Q_N\left(\boldsymbol{x}\right)\Big) &\leqslant \frac{2}{N}\Big(|x_1 - x_{01}| + |x_2 - x_{02}|\Big) \\
&\leqslant \frac{2\sqrt{2}}{N}\ \|\boldsymbol{x}_0 - \boldsymbol{x}\|\ ,
\end{aligned}$$

so that $\left| f^{(Q)}_N\left(\boldsymbol{x}_0\right) - f^{(Q)}_N\left(\boldsymbol{x}\right)\right| \leqslant 2\sqrt{2}\ N\ \|f\|_\infty\ \|\boldsymbol{x}_0 - \boldsymbol{x}\|$, which proves the continuity of $f^{(Q)}_N$, while uniform continuity comes from $\mathbb{T}^2$ being compact.

Concerning the norm in (36), the upper bound $\|\Gamma_N\|_{\mathcal{B}} \leqslant 1$ is clear and the maximum is reached by choosing f constant. ■

By means of the RAO, the discretization operator in (33) can be conveniently written as

$$\mathcal{J}_{\mathcal{N},\infty}(f) = \sum_{\boldsymbol{\ell} \in (\mathbb{Z}/N\mathbb{Z})^2} f^{(Q)}_N\left(\frac{\boldsymbol{\ell}}{N}\right) |\boldsymbol{\ell}\rangle\langle\boldsymbol{\ell}|\ \cdot \tag{37}$$

Analogously, the de–discretization operator in (34) can be recast as

$$\mathcal{J}_{\infty,\mathcal{N}}(X)(\boldsymbol{x}) = \sum_{\boldsymbol{\ell}\in(\mathbb{Z}/N\mathbb{Z})^2} X_{\boldsymbol{\ell},\boldsymbol{\ell}} \;\; \delta^{(N)}_{\boldsymbol{\ell}\,,\,\hat{\boldsymbol{x}}_N} \;\; = \sum_{\boldsymbol{\ell}\in(\mathbb{Z}/N\mathbb{Z})^2} X_{\boldsymbol{\ell},\boldsymbol{\ell}} \, \mathcal{X}_{Q_N\left(\frac{\boldsymbol{\ell}}{N}\right)}(\boldsymbol{x}) \;, \tag{38}$$

thus proving that $\mathrm{Ran}\left(\mathcal{J}_{\infty,\mathcal{N}}\right) = \mathcal{S}\left(\mathbb{T}^2\right)$.

Moreover, combining equations (37) and (38), we explicitly get the simple function arising from $f \in L^\infty_\mu\left(\mathbb{T}^2\right)$, via AW discretization/de–discretization:

$$\left(\mathcal{J}_{\infty,\mathcal{N}} \circ \mathcal{J}_{\mathcal{N},\infty}\right)(f)(\boldsymbol{x}) = \sum_{\boldsymbol{\ell}\in(\mathbb{Z}/N\mathbb{Z})^2} \Gamma_N\left(f\right)\left(\frac{\boldsymbol{\ell}}{N}\right) \; \mathcal{X}_{Q_N\left(\frac{\boldsymbol{\ell}}{N}\right)}(\boldsymbol{x}) \;\cdot \tag{39}$$

The action of the operator $\mathcal{J}_{\infty,\mathcal{N}} \circ \mathcal{J}_{\mathcal{N},\infty}$ can be seen in Figures 4 and 5.

B. Proof of Proposition 5.1

We start by proving the inclusions (22).

For every real number t, we have $0 \leqslant \left\langle Nt + \frac{1}{2}\right\rangle = Nt + \frac{1}{2} - \left\lfloor Nt + \frac{1}{2}\right\rfloor < 1$, so that

$$\left| t - \frac{\left\lfloor Nt + \frac{1}{2}\right\rfloor}{N}\right| \leqslant \frac{1}{2N} \qquad , \qquad \forall\, t \in \mathbb{R}\cdot$$

From (5) in Definition 3.2, we derive

$$d_{\mathbb{T}^2}\left(\boldsymbol{x}\;,\;\frac{\hat{\boldsymbol{x}}_N}{N}\right) \leqslant \frac{1}{\sqrt{2}N} \qquad , \qquad \forall\, \boldsymbol{x} \in \mathbb{T}^2\cdot \tag{40}$$

Then, let us consider the triangular inequality

$$d_{\mathbb{T}^2}\left(\boldsymbol{x}\;,\;\boldsymbol{y}\right) \leqslant d_{\mathbb{T}^2}\left(\boldsymbol{x}\;,\;\frac{\hat{\boldsymbol{x}}_N}{N}\right) + d_{\mathbb{T}^2}\left(\frac{\hat{\boldsymbol{x}}_N}{N}\;,\;\boldsymbol{y}\right) \qquad \forall\, \boldsymbol{y} \in \mathbb{T}^2 \qquad , \tag{41}$$

and let us take the infimum over the set $\boldsymbol{y} \in \Gamma_n$ defined in (17)

$$\begin{aligned} d_{\mathbb{T}^2}\left(\frac{\hat{\boldsymbol{x}}_N}{N}\;,\;\Gamma_n\right) &\geqslant d_{\mathbb{T}^2}\left(\boldsymbol{x}\;,\;\Gamma_n\right) - d_{\mathbb{T}^2}\left(\boldsymbol{x}\;,\;\frac{\hat{\boldsymbol{x}}_N}{N}\right) \\ &\geqslant d_{\mathbb{T}^2}\left(\boldsymbol{x}\;,\;\Gamma_n\right) - \frac{1}{\sqrt{2}N}\;, \end{aligned}$$

where we used (40). Therefore, considering the complement $\left[\overline{\Gamma}_n(\varepsilon)\right]^\circ$ of the union of strip of width ε, $\overline{\Gamma}_n(\varepsilon)$ defined in (19), we get that

$$\boldsymbol{x} \in \left[\overline{\Gamma}_n(\varepsilon)\right]^\circ \quad \Longrightarrow \quad \frac{\hat{\boldsymbol{x}}_N}{N} \in \left[\overline{\Gamma}_n\left(\varepsilon - \frac{1}{\sqrt{2}N}\right)\right]^\circ .$$

Further, from (20), it follows that, if the lattice point $\frac{\hat{\boldsymbol{x}}_N}{N}$ does not belong to $\overline{\Gamma}_n\left(\varepsilon - \frac{1}{\sqrt{2}N}\right)$, then the corresponding point $\boldsymbol{x} \in \mathbb{T}^2$ must belong to $G_n^N\left(\varepsilon - \frac{1}{\sqrt{2}N}\right)$.
Changing $\varepsilon - \frac{1}{\sqrt{2}N} \longmapsto \varepsilon$ we obtain the first inclusion relation in equation (22); the second one follows by interchanging the role played by $\frac{\hat{\boldsymbol{x}}_N}{N}$ and $\boldsymbol{x}$ in (41).

In order to prove (23) , we start by considering the matrices $S_\alpha = \left(\begin{smallmatrix} 1+\alpha & 1 \\ \alpha & 1 \end{smallmatrix}\right)$ and its inverse $S_\alpha^{-1} = \left(\begin{smallmatrix} 1 & -1 \\ -\alpha & 1+\alpha \end{smallmatrix}\right)$. Let η be the largest (positive) eigenvalue of $\sqrt{S_\alpha^\dagger S_\alpha}$; its characteristic polynomial for η is $\eta^4 - \left(2\,\alpha^2 + 2\,\alpha + 3\right)\eta^2 + 1 = 0$, whence η attains its minimum $\eta_{\min} = \sqrt{2}$ at $\alpha = -\frac{1}{2}$. Then, we set $\widetilde{N} := 2\sqrt{2}\left(\sqrt{2}+1\right)\eta^{2n}$, $n \in \mathbb{N}$, choose $N > \widetilde{N}$ and proceed by induction.

$\boldsymbol{p = 0}:$ from definitions (10) and (11), it follows

$$d_{\mathbb{T}^2}\left(\frac{U_\alpha^0(N\boldsymbol{x})}{N}, \frac{V_\alpha^0(\hat{\boldsymbol{x}}_N)}{N}\right) = d_{\mathbb{T}^2}\left(\boldsymbol{x}, \frac{\hat{\boldsymbol{x}}_N}{N}\right) < \frac{1}{\sqrt{2}N} < \frac{\sqrt{2}}{N} ,$$

where the first inequality follows from (40), thus relation (23) holds for $p = 0$.

$\boldsymbol{p = q - 1,\ 1 \leqslant q \leqslant n}:$ since

$$d_{\mathbb{T}^2}\left(\frac{U_\alpha^q(N\boldsymbol{x})}{N}, \frac{V_\alpha^q(\hat{\boldsymbol{x}}_N)}{N}\right) \leqslant d_{\mathbb{T}^2}\left(\frac{U_\alpha\left(U_\alpha^{q-1}(N\boldsymbol{x})\right)}{N}, \frac{U_\alpha\left(V_\alpha^{q-1}(\hat{\boldsymbol{x}}_N)\right)}{N}\right) + \\ + d_{\mathbb{T}^2}\left(\frac{U_\alpha\left(V_\alpha^{q-1}(\hat{\boldsymbol{x}}_N)\right)}{N}, \frac{V_\alpha\left(V_\alpha^{q-1}(\hat{\boldsymbol{x}}_N)\right)}{N}\right) ,$$

using (10) in the first term and noting that, from definitions (10) and (11), the second term is less or equal to $\frac{\sqrt{2}}{N}$, we get

$$d_{\mathbb{T}^2}\left(\frac{U_\alpha^q(N\boldsymbol{x})}{N}, \frac{V_\alpha^q(\hat{\boldsymbol{x}}_N)}{N}\right) \leqslant d_{\mathbb{T}^2}\left(S_\alpha\left(\frac{U_\alpha^{q-1}(N\boldsymbol{x})}{N}\right), S_\alpha\left(\frac{V_\alpha^{q-1}(\hat{\boldsymbol{x}}_N)}{N}\right)\right) + \frac{\sqrt{2}}{N} .$$

By the induction hypothesis we have:

$$d_{\mathbb{T}^2}\left(\frac{U_\alpha^{q-1}(N\boldsymbol{x})}{N},\frac{V_\alpha^{q-1}(\hat{\boldsymbol{x}}_N)}{N}\right)\leqslant\frac{\sqrt{2}}{N}\left(\frac{\eta^q-1}{\eta-1}\right) \tag{42}$$

$$\leqslant\frac{\sqrt{2}}{N}\,\frac{1}{\sqrt{2}-1}\,\eta^q$$

$$\left(\eta>\sqrt{2}\ ,\ 1\leqslant q\leqslant n\quad\Longrightarrow\right)\qquad<\frac{1}{2}\,\eta^{q-2n}<\frac{1}{2}\eta^{-1}\ . \tag{43}$$

Now we set $\varepsilon=\frac{\widetilde{N}}{2N}$, taking into account that $\eta\geqslant\sqrt{2}$ and use the right inclusion in (22) to deduce that

$$\boldsymbol{x}\in G_n^N\left(\frac{\widetilde{N}}{2N}\right)\Longrightarrow\boldsymbol{x}\notin\overline{\Gamma}_n\left(\frac{\widetilde{N}}{2N}-\frac{1}{\sqrt{2}N}\right)\ .$$

At this point, we make use of the following result, which shall be proved in Lemma B.1.3: it states that if a point does not belong to $\overline{\Gamma}_n(\varepsilon)$, the union of the the strips of width $\varepsilon\leqslant\frac{1}{2}$ up to time n, then its orbit under S_α up to time $n-1$ is farther away than $\varepsilon\eta^{-q},0\leqslant q<n$ from the discontinuity line γ_0. Explicitly

$$\boldsymbol{x}\notin\overline{\Gamma}_n(\varepsilon)\Longrightarrow d_{\mathbb{T}^2}\left(S_\alpha^q(\boldsymbol{x}),\gamma_0\right)>\varepsilon\,\eta^{-q}\ ,\ \forall\ 0\leqslant q<n\ ,$$

whence

$$d_{\mathbb{T}^2}\left(\frac{U_\alpha^{q-1}(N\boldsymbol{x})}{N},\gamma_0\right)>\left(\frac{\widetilde{N}}{2N}-\frac{1}{\sqrt{2}N}\right)\eta^{1-q}$$

$$>\frac{\sqrt{2}}{N}\left(\frac{\eta^{2n-1}-\eta^{q-1}}{\eta-1}\right)\eta^{1-q}$$

$$\geqslant\frac{\sqrt{2}}{N}\left(\frac{\eta^q-1}{\eta-1}\right)\ , \tag{44}$$

where the second inequality comes from $\eta\geqslant\sqrt{2}$, the relation $\dfrac{\eta^n-1}{\eta-1}\leqslant\dfrac{1}{\sqrt{2}-1}\,\eta^n$ and the following estimates:

$$
\begin{aligned}
\left(\frac{\widetilde{N}}{2N} - \frac{1}{\sqrt{2}N}\right) &= \frac{\sqrt{2}}{N}\left(\left(\sqrt{2}+1\right)\eta^{2n} - \frac{1}{2}\right) \\
&\geqslant \frac{\sqrt{2}}{N}\left[\left(\sqrt{2}+1\right)\left(\sqrt{2}-1\right)\frac{\eta^{2n}-\eta+\eta-1}{\eta-1} - \frac{1}{2}\right] \\
&\geqslant \frac{\sqrt{2}}{N}\left[\eta\,\frac{\eta^{2n-1}-1}{\eta-1} + \frac{1}{2}\right] \geqslant \frac{\sqrt{2}}{N}\left(\frac{\eta^{2n-1}-\eta^{q-1}}{\eta-1}\right) \cdot
\end{aligned}
$$

Therefore, comparing (44) with (42)

$$
d_{\mathbb{T}^2}\left(\frac{U_\alpha^{q-1}\left(N\boldsymbol{x}\right)}{N}, \frac{V_\alpha^{q-1}\left(\hat{\boldsymbol{x}}_N\right)}{N}\right) < d_{\mathbb{T}^2}\left(\frac{U_\alpha^{q-1}\left(N\boldsymbol{x}\right)}{N}, \gamma_0\right) \quad , \quad \forall q \leqslant n \cdot
$$

As a consequence, the segment $\left(\frac{U_\alpha^{q-1}(N\boldsymbol{x})}{N}, \frac{V_\alpha^{q-1}(\hat{\boldsymbol{x}}_N)}{N}\right)$ cannot cross the line γ_0. This condition, together with (43), allows us to use another result proved in Lemma B.1.1b, which states that if a segment (A, B) on the torus does not cross the discontinuity line γ_0 then $d_{\mathbb{T}^2}\left(S_\alpha\left(A\right), S_\alpha\left(B\right)\right) \leqslant \eta\, d_{\mathbb{T}^2}\left(A, B\right)$. We can finally conclude with:

$$
d_{\mathbb{T}^2}\left(\frac{U_\alpha^{q}\left(N\boldsymbol{x}\right)}{N}, \frac{V_\alpha^{q}\left(\hat{\boldsymbol{x}}_N\right)}{N}\right) \leqslant \eta\frac{\sqrt{2}}{N}\left(\frac{\eta^{q}-1}{\eta-1}\right) + \frac{\sqrt{2}}{N} = \frac{\sqrt{2}}{N}\left(\frac{\eta^{q+1}-1}{\eta-1}\right) \cdot \qquad \blacksquare
$$

The following Lemma, which has been used in the proof of the previous Proposition, deals with the geometrical properties of the Sawtooth dynamics.

Lemma B.1

With η the largest (positive) eigenvalue of $\sqrt{S_\alpha^\dagger S_\alpha}$ and $A, B \in \mathbb{T}^2$ such that $d_{\mathbb{T}^2}\left(A, B\right) < \frac{1}{2}\,\eta^{-1}$, it follows:

(1a) If the segment (A, B) does not cross γ_{-1}, then

$$
d_{\mathbb{T}^2}\left(S_\alpha^{-1}\left(A\right), S_\alpha^{-1}\left(B\right)\right) \leqslant \eta\, d_{\mathbb{T}^2}\left(A, B\right) \cdot \tag{45a}
$$

(1b) If (A, B) does not cross γ_0, then

$$
d_{\mathbb{T}^2}\left(S_\alpha\left(A\right), S_\alpha\left(B\right)\right) \leqslant \eta\, d_{\mathbb{T}^2}\left(A, B\right) \cdot \tag{45b}
$$

(2) For any given $\alpha \in \mathbb{R}$, $p \in \mathbb{N}^+$ and $0 \leqslant \varepsilon \leqslant \frac{1}{2}\eta^{-1}$,

$$\boldsymbol{x} \in \overline{\gamma}_{p-1}(\varepsilon) \Longrightarrow S_\alpha^{-1}(\boldsymbol{x}) \in \left(\overline{\gamma}_p(\eta\,\varepsilon) \cup \overline{\gamma}_0(\eta\,\varepsilon)\right) \cdot$$

(3) For any given $\alpha \in \mathbb{R}$, $n \in \mathbb{N}^+$ and $0 \leqslant \varepsilon \leqslant \frac{1}{2}$, with U_α^q as in (10),

$$\boldsymbol{x} \notin \overline{\Gamma}_n(\varepsilon) \Longrightarrow d_{\mathbb{T}^2}\left(\frac{U_\alpha^q(N\boldsymbol{x})}{N}, \gamma_0\right) > \varepsilon\,\eta^{-q}\ ,\ \forall\ 0 \leqslant q < n \cdot$$

Proof:

In the course of the proof, we shall use that

$$\left\| S_\alpha^{\pm 1} \cdot \boldsymbol{v} \right\|_{\mathbb{R}^2} \leqslant \eta \quad \|\boldsymbol{v}\|_{\mathbb{R}^2}\ , \tag{46a}$$

$$\left\| S_\alpha^{\pm 1} \cdot \boldsymbol{v} \right\|_{\mathbb{R}^2} \geqslant \eta^{-1}\|\boldsymbol{v}\|_{\mathbb{R}^2}\ , \tag{46b}$$

which directly follows from the definition of η, where $\boldsymbol{v}$ is any 2–dimensional real vector.

In order to prove (45), it is convenient to unfold $\mathbb{T}^2$ and the discontinuity of S_α on the plane $\mathbb{R}^2$. This is most easily done as follows. Points $A \in \mathbb{T}^2 = \mathbb{R}^2/\mathbb{Z}^2$ are represented by equivalence classes

$$[\boldsymbol{a}] := \left\{\boldsymbol{a} + \boldsymbol{n}\ ,\ \boldsymbol{n} \in \mathbb{Z}^2\right\}\ ,\ \boldsymbol{a} \in [0,1)^2 \cdot \tag{47}$$

Given $A, B \in \mathbb{T}^2$, let $A^b \in [\boldsymbol{a}]$ be such that

$$d_{\mathbb{T}^2}([\boldsymbol{a}], [\boldsymbol{b}]) = \left\| A^b - \boldsymbol{b} \right\|_{\mathbb{R}^2} \cdot$$

Notice that

$$d_{\mathbb{T}^2}([\boldsymbol{a}], [\boldsymbol{b}]) = \|\boldsymbol{a} - \boldsymbol{b}\|_{\mathbb{R}^2} \quad \text{iff} \quad \|\boldsymbol{a} - \boldsymbol{b}\|_{\mathbb{R}^2} \leqslant \frac{1}{2} \tag{48}$$

(1a) (A, B) not crossing γ_{-1} means that the segment $\left(A^b, \boldsymbol{b}\right)$ does not intersect γ_{-1}. Periodically covering the plane–$\mathbb{R}^2$ by squares $[0,1)^2$, the γ_{-1}-lines form a set of (parallel) straight lines $x_1 - x_2 = n \in \mathbb{Z}$; it follows that $\left(A^b, \boldsymbol{b}\right)$ does not cross γ_{-1} iff

$$\left\lfloor A_1^b - A_2^b \right\rfloor = \lfloor b_1 - b_2 \rfloor\ , \tag{49}$$

where the integral part on the r.h.s. takes values $0, -1$, depending on which side of the diagonal γ_{-1} the point $\boldsymbol{b}$ lies within.

As $S_\alpha^{\pm}$ are not sensitive to the integer part of their arguments, their actions are the same on all elements of the equivalence classes (47), that is

$$d_{\mathbb{T}^2}\left(S_\alpha^{-1}(A), S_\alpha^{-1}(B)\right) = d_{\mathbb{T}^2}\left(S_\alpha^{-1}([\boldsymbol{a}]), S_\alpha^{-1}([\boldsymbol{b}])\right) = d_{\mathbb{T}^2}\left(S_\alpha^{-1}\left(A^b\right), S_\alpha^{-1}(\boldsymbol{b})\right) \ \cdot$$

By expanding $\langle x\rangle = x - \lfloor x\rfloor$, using the definition of $S_\alpha^{-1}(\cdot)$ and putting together all integral contributions, condition (49) yields

$$\begin{aligned} d_{\mathbb{T}^2}\left(S_\alpha^{-1}(A), S_\alpha^{-1}(B)\right) &= \min_{\boldsymbol{m}\in\mathbb{Z}^2} \left\| S_\alpha^{-1}(A) - S_\alpha^{-1}(B) + \boldsymbol{m}\right\|_{\mathbb{R}^2} \\ &= \min_{\boldsymbol{m'}\in\mathbb{Z}^2} \left\| S_\alpha^{-1}\cdot\left(A^b - \boldsymbol{b}\right) + \boldsymbol{m'}\right\|_{\mathbb{R}^2} \\ &= d_{\mathbb{T}^2}\left(S_\alpha^{-1}\cdot\left(A^b - \boldsymbol{b}\right), 0\right) \ \cdot \end{aligned}$$

Applying (46a), since we assumed $d_{\mathbb{T}^2}(A,B) < \frac{1}{2}\,\eta^{-1}$, we estimate

$$\begin{aligned} &\left\| S_\alpha^{-1}\cdot\left(A^b - \boldsymbol{b}\right)\right\|_{\mathbb{R}^2} \leqslant \eta \left\| A^b - \boldsymbol{b}\right\|_{\mathbb{R}^2} \\ &= \eta\, d_{\mathbb{T}^2}(A,B) < \frac{1}{2} \ \cdot \end{aligned}$$

In particular, using (48), the previous inequalities imply

$$d_{\mathbb{T}^2}\left(S_\alpha^{-1}\cdot\left(A^b - \boldsymbol{b}\right), 0\right) = \left\| S_\alpha^{-1}\cdot\left(A^b - \boldsymbol{b}\right)\right\|_{\mathbb{R}^2} \leqslant \eta\, d_{\mathbb{T}^2}(A,B) \ \cdot$$

(1b) Using the same argument as (1a), the union of γ_0-lines constitute a set of straight lines $x_1 = n \in \mathbb{Z}$; Therefore the segment $\left(A^b, \boldsymbol{b}\right)$ does not cross γ_0 iff

$$\left\lfloor A_1^b \right\rfloor = \lfloor b_1 \rfloor \ \cdot \tag{50}$$

As done before, by means of (50), we arrive at

$$d_{\mathbb{T}^2}\left(S_\alpha(A), S_\alpha(B)\right) = d_{\mathbb{T}^2}\left(S_\alpha\left(A^b\right), S_\alpha(\boldsymbol{b})\right) = d_{\mathbb{T}^2}\left(S_\alpha\cdot\left(A^b - \boldsymbol{b}\right), 0\right) \ \cdot$$

The proof can now be completed exactly as for point (2a) before.

(2) We denote by $d_{\mathbb{T}^2}(\boldsymbol{x},\gamma) = \inf_{\boldsymbol{y}\in\gamma} d_{\mathbb{T}^2}(\boldsymbol{x},\boldsymbol{y})$ the distance of the point $\boldsymbol{x}\in\mathbb{T}^2$ from a curve $\gamma\in\mathbb{T}^2$. Then, from Definition (18) we have:

$$\boldsymbol{x} \in \overline{\gamma}_{p-1}(\varepsilon) \Longrightarrow \varepsilon \geqslant d_{\mathbb{T}^2}(\boldsymbol{x},\gamma_{p-1}) = d_{\mathbb{T}^2}(\boldsymbol{x},\boldsymbol{y}^\star) \ , \tag{51}$$

where $\boldsymbol{y}^\star$ is the nearest point to $\boldsymbol{x}$ belonging to γ_{p-1}.
We distinguish two cases:

(2′) The segment $(\boldsymbol{x}, \boldsymbol{y}^\star)$ does not cross[1] γ_{-1}

From (51) and point (1a), since $S_\alpha^{-1}(\boldsymbol{y}^\star) \in \gamma_p$ (see (16a)), we get

$$\begin{aligned} d_{\mathbb{T}^2}\left(S_\alpha^{-1}(\boldsymbol{x}), \gamma_p\right) &\leqslant d_{\mathbb{T}^2}\left(S_\alpha^{-1}(\boldsymbol{x}), S_\alpha^{-1}(\boldsymbol{y}^\star)\right) \\ &\leqslant \eta\, d_{\mathbb{T}^2}(\boldsymbol{x}, \boldsymbol{y}^\star) \leqslant \eta\, \varepsilon \cdot \end{aligned}$$

Therefore $S_\alpha^{-1}(\boldsymbol{x}) \in \overline{\gamma}_p(\eta\, \varepsilon)$.

(2″) The segment $(\boldsymbol{x}, \boldsymbol{y}^\star)$ crosses γ_{-1}.
In this case, there exists $\boldsymbol{z} \in \gamma_{-1}$ such that

$$d_{\mathbb{T}^2}(\boldsymbol{x}, \boldsymbol{y}^\star) = d_{\mathbb{T}^2}(\boldsymbol{x}, \boldsymbol{z}) + d_{\mathbb{T}^2}(\boldsymbol{z}, \boldsymbol{y}^\star) \ \cdot \tag{52}$$

Then, from (51) and (52),

$$\varepsilon \geqslant d_{\mathbb{T}^2}(\boldsymbol{x}, \boldsymbol{y}^\star) \geqslant d_{\mathbb{T}^2}(\boldsymbol{x}, \boldsymbol{z}) \ \cdot$$

Since, according to (16), $S_\alpha^{-1}(\boldsymbol{z}) \in \gamma_0$, from point (1a) we get

$$d_{\mathbb{T}^2}\left(S_\alpha^{-1}(\boldsymbol{x}), \gamma_0\right) \leqslant d_{\mathbb{T}^2}\left(S_\alpha^{-1}(\boldsymbol{x}), S_\alpha^{-1}(\boldsymbol{z})\right) \leqslant \eta\, \varepsilon \ ,$$

that is $S_\alpha^{-1}(\boldsymbol{x}) \in \overline{\gamma}_0(\eta\, \varepsilon)$.

(3) From point (2), it follows that, when $0 \leqslant \varepsilon \leqslant \frac{1}{2}$, for $p \in \mathbb{N}^+$,

$$\boldsymbol{x} \notin \left(\overline{\gamma}_p(\varepsilon) \cup \overline{\gamma}_0(\varepsilon)\right) \Longrightarrow S_\alpha(\boldsymbol{x}) \notin \overline{\gamma}_{p-1}\left(\eta^{-1}\varepsilon\right) \ \cdot \tag{53}$$

We prove by induction that, when $0 \leqslant \varepsilon \leqslant \frac{1}{2}$, for $m \in \mathbb{N}^+$,

$$\boldsymbol{x} \notin \bigcup_{p=0}^{m} \overline{\gamma}_p(\varepsilon) \Longrightarrow S_\alpha(\boldsymbol{x}) \notin \bigcup_{p=0}^{m-1} \overline{\gamma}_p\left(\eta^{-1}\varepsilon\right) \ \cdot \tag{54}$$

For $m = 1$, (54) follows from (53); if (54) holds for $m = r$, then take

$$\boldsymbol{x} \notin \bigcup_{p=0}^{r+1} \overline{\gamma}_p(\varepsilon) \ . \text{ This means that } \quad \boldsymbol{x} \notin \bigcup_{p=0}^{r} \overline{\gamma}_p(\varepsilon) \quad \text{and} \quad \boldsymbol{x} \notin \left(\overline{\gamma}_{r+1}(\varepsilon) \cup \overline{\gamma}_0(\varepsilon)\right) \ \cdot$$

[1] we stipulate that, if $\boldsymbol{y}^\star \in \gamma_{-1}$ or $\boldsymbol{x} \in \gamma_{-1}$, we are still in a non–crossing condition

Now, using the induction hypothesis and (53), we get

$$\boldsymbol{x} \notin \bigcup_{p=0}^{r+1} \overline{\gamma}_p\left(\varepsilon\right) \Longrightarrow S_\alpha\left(\boldsymbol{x}\right) \notin \bigcup_{p=0}^{r-1} \overline{\gamma}_p\left(\eta^{-1}\varepsilon\right) \quad \text{and} \quad S_\alpha\left(\boldsymbol{x}\right) \notin \overline{\gamma}_r\left(\eta^{-1}\varepsilon\right) \cdot$$

Setting $m = n-1$ and iterating q times the implication (54) argument, we get

$$\boldsymbol{x} \notin \bigcup_{p=0}^{n-1} \overline{\gamma}_p\left(\varepsilon\right) \Longrightarrow S_\alpha^q\left(\boldsymbol{x}\right) \notin \bigcup_{p=0}^{n-1-q} \overline{\gamma}_p\left(\eta^{-q}\varepsilon\right) \quad , \quad \forall\ 0 \leqslant q < n \cdot$$

In particular $S_\alpha^q\left(\boldsymbol{x}\right) \notin \overline{\gamma}_0\left(\eta^{-q}\varepsilon\right)$, which leads to the lower bound

$$d_{\mathbb{T}^2}\left(S_\alpha^q\left(\boldsymbol{x}\right), \gamma_0\right) > \eta^{-q}\varepsilon \quad , \quad \forall\ 0 \leqslant q < n \ ,$$

whence the result follows in view of Definitions (10) and (19). ■

C. Proof of Proposition 5.2

(a) In (16a), we have defined $\gamma_p = S_\alpha^{-p}\left(\gamma_0\right)$ where $S_\alpha^{-1}\left(\boldsymbol{x}\right)$ (as well as $S_\alpha^{-p}\left(\boldsymbol{x}\right)$) is a piecewise continuous mapping onto $\mathbb{T}^2$ with jump–discontinuities across the γ_p lines due to the presence of the function $\langle\cdot\rangle$ in (9). Away from the discontinuities, $S_\alpha^{-p}\left(\boldsymbol{x}\right)$ behaves as the matrix action $S_\alpha^{-p} \cdot \boldsymbol{x}$. We want now to estimate the length $l\left(\gamma_p\right)$; in order to do that, we unfold γ_p on the plane and calculate the length of the segment $\left\{\boldsymbol{x} \in \mathbb{R}^2 \;\middle|\; \boldsymbol{x} = S_\alpha^{-p} \cdot \binom{0}{y} \ , \ y \in [0,1)\right\}$, which, in its turn, is the image of γ_0 under the matrix action given by $S_\alpha^{-p} \cdot \boldsymbol{x}$. Therefore, using (46a), the result follows.

(b) Let $\overline{L}\left(\varepsilon\right)$ denote the set of points having distance from a segment of length L smaller or equal than ε: it has a volume (under the Lebesgue measure μ) given by

$$\mu\left(\overline{L}\left(\varepsilon\right)\right) = 2\,L\,\varepsilon + \pi\varepsilon^2 \ ,$$

where the last term on the r.h.s. takes into account rounding of the extremes of the strip by to semi–circle of radius ε. Then (29b) follows from (29a).

(c) This follows from Definition (19):

$$\mu\left(\overline{\Gamma}_n(\varepsilon)\right) = \mu\left(\bigcup_{p=0}^{n-1} \overline{\gamma}_p(\varepsilon)\right) \leqslant \sum_{p=0}^{n-1} \mu\left(\overline{\gamma}_p(\varepsilon)\right) \ .$$

Using (29b), we can write:

$$\mu\left(\overline{\Gamma}_n(\varepsilon)\right) \leqslant 2\,\varepsilon \sum_{p=0}^{n-1} \eta^p + \sum_{p=0}^{n-1} \pi\,\varepsilon^2 = 2\,\varepsilon\,\frac{\eta^n - 1}{\eta\ - 1} + n\,\pi\,\varepsilon^2 \ .$$

Finally, the estimate $\dfrac{x^p - 1}{x\ - 1} \leqslant \left(\sqrt{2}+1\right) x^p$, valid for $x > \sqrt{2}$, yields

$$\mu\left(\overline{\Gamma}_n(\varepsilon)\right) \leqslant 2\,\varepsilon\left(\sqrt{2}+1\right)\eta^n + n\,\pi\,\varepsilon^2 \qquad\qquad .$$

(d) By writing the left inclusion in (22) in terms of complementary sets, with $\varepsilon = \frac{\widetilde{N}}{2N}$, we get:

$$\left[G_n^N\left(\frac{\widetilde{N}}{2N}\right)\right]^\circ \subseteq \overline{\Gamma}_n\left(\frac{\widetilde{N}}{2N} + \frac{1}{\sqrt{2}N}\right) \text{ and so}$$

$$\mu\left(\left[G_n^N\left(\frac{\widetilde{N}}{2N}\right)\right]^\circ\right) \leqslant \mu\left(\overline{\Gamma}_n\left(\frac{\widetilde{N}}{2N} + \frac{1}{\sqrt{2}N}\right)\right) \ .$$

By substituting in (29c) $\frac{\widetilde{N}+\sqrt{2}}{2N} = \frac{\widetilde{N}}{2N} + \frac{1}{\sqrt{2}N}$ in the place of ε, we get:

$$\mu\left(\left[G_n^N\left(\frac{\widetilde{N}}{2N}\right)\right]^\circ\right) \leqslant \frac{\widetilde{N}+\sqrt{2}}{2N}\left(\sqrt{2}+1\right)\left(2\,\eta^n + \frac{n}{\sqrt{2}+1}\,\pi\,\frac{\widetilde{N}+\sqrt{2}}{2N}\right) \ . \tag{55}$$

Finally, the r.h.s of (55), can be estimated by the following upper bounds:

$$\begin{aligned} \pi\,\frac{\widetilde{N}+\sqrt{2}}{2N} &< 2 \\ \frac{n}{\sqrt{2}+1} &< \eta^n \\ \left(\widetilde{N}+\sqrt{2}\right)\left(\sqrt{2}+1\right) &< 19\,\eta^{2n} \end{aligned}$$

which hold for $\forall\ N > \widetilde{N},\ \eta \geqslant \sqrt{2}$ and $\forall\ n \in \mathbb{N}^+$. This ends the proof. ∎

References

[1] G.M. Zaslavsky, *Chaos in Dynamic Systems*, Harwood Academic Publ., Chur, 1985.

[2] M.–J. Giannoni, A. Voros and J. Zinn–Justin, editors, *Chaos and Quantum Physics*, volume 1989 Les Houches Session LII of *Les Houches Summer School of Theoretical Physics*, Amsterdam, The Netherlands, 1991, North–Holland.

[3] G. Casati and B. Chirikov, *Quantum Chaos. Between Order and Disorder*, Cambridge University Press, Cambridge, 1995.

[4] R. Devaney, *An Introduction to Chaotic Dynamical Systems*, Addison–Wesley, Reading, MA, 1989.

[5] S. Wiggins, *Dynamical Systems and Chaos*, Springer–Verlag, New York, 1990.

[6] A. Katok and B. Hasselblatt, *Introduction to the Modern Theory of Dynamical Systems*, Encyclopedia of Mathematics and its Applications, Cambridge University Press, Cambridge, 1999.

[7] J. M. Bouclet and S. De Bievre, Long time propagation and control on scarring for perturbed quantized hyperbolic toral automorphisms, *Preprint* `math-ph/0409069`, 2004.

[8] A. Fannjiang, S. Nonnenmacher and L. Wolowski, Dissipation time of quantized toral maps, *Preprint* `math-ph/0406055`, 2004.

[9] R. Schubert, Semiclassical behavior of expectation values in time evolved lagrangian states for large times, *Preprint* `math.MP/0402038`, 2004.

[10] V. Cappellini, *Quantum Dynamical Entropies and Complexity in Dynamical Systems*, PhD thesis, University of Trieste, 2004, *Preprint* `math-ph/0403035`.

[11] A. Crisanti, M. Falcioni and A. Vulpiani, Transition from regular to complex behavior in a discrete deterministic asymmetric neural network model, *J. Phys. A: Math. Gen.* **26**, 3441 (1993).

[12] A. Crisanti, M. Falcioni, G. Mantica and A. Vulpiani, Applying algorithmic complexity to define chaos in the motion of complex systems, *Phys. Rev. E* **50(3)**, 1959–1967 (1994).

[13] M. Falcioni, G. Mantica, S. Pigolotti and Vulpiani A., Coarse-grained probabilistic automata mimicking chaotic systems, *Phys. Rev. Lett.* **91(4)**, 044101 (2003).

[14] F. Benatti, V. Cappellini and F. Zertuche, Quantum dynamical entropies in discrete classical chaos, *J. Phys. A: Math. Gen.* **37(1)**, 105–130 (2004).

[15] J. Marklof and S. O'Keefe, Weyl's law and quantum ergodicity for maps with divided phase space, *Nonlinearity* **18**, 277–304 (2005).

[16] N. Chernoff, Ergodic and statistical properties of piecewise linear hyperbolic automorphisms of the two-torus, *J. Stat. Phys.* **69**, 111–134 (1992).

[17] S. Vaienti, Ergodic properties of the discontinuous sawtooth map, *J. Stat. Phys.* **67**, 251–269 (1992).

[18] I. C. Percival and F. Vivaldi, A linear code for the sawtooth and cat maps, *Physica D* **27**, 373 (1987).

[19] F. Bonechi and S. De Bièvre, Controlling strong scarring for quantized ergodic toral automorphisms, *Duke Math. J.* **3**, 571–587 (2003).

[20] O. Bratteli and D. W. Robinson, *Operator algebras and quantum statistical mechanics (v.1: C*- and W*-algebras, symmetry groups, decomposition of states)*, Texts and monographs in physics, Springer–Verlag, New York, 1979.

[21] E. Hewitt and K. Stromberg, *Real and Abstract Analysis*, Springer–Verlag, Berlin, 2nd edition, 1969.

[22] M. V. Berry and J. H. Hannay, Quantization of linear maps on a torus – Fresnel diffraction by a periodic grating, *Physica D* **1**, 267–290 (1980).

[23] M. Degli Esposti, Quantization of the orientation preserving automorphisms of the torus, *Ann. Inst. Henri Poincaré* **58**, 323–34 (1993).

[24] J. Marklof and Z. Rudnick, Quantum unique ergodicity for parabolic maps, *Preprint* `math-ph/9901001`, 1999.

[25] F. Benatti, V. Cappellini, M. De Cock, M. Fannes and D. Vanpeteghem, Classical limit of quantum dynamical entropies, *Rev. Math. Phys.* **15(8)**, 847–875 (2003).

[26] J. Ford, G. Mantica and G.H. Ristow, The Arnold cat-failure of the correspondence principle, *Physica D* **50**, 493–520 (1991).

[27] T. M. Apostol, *Introduction to analytic number theory*, Undergraduate Texts in Mathematics, Springer–Verlag, New York, NY, 1976.

[28] V. Cappellini, Quantum dynamical entropies for discrete classical systems: a comparison, *J. Phys. A: Math. Gen.* **38(31)**, 6893–6915 (2005).

[29] W. Słomczyński and K. Życzkowski, Quantum chaos: an entropy approach, *J. Math. Phys.* **35(11)**, 5674–5700 (1994).

[30] W. Rudin, *Real and Complex Analysis*, McGraw–Hill, New York, 3rd edition, 1987.

[31] F Riesz and B. Sz.–Nagy, *Functional Analysis*, Frederick Ungar Publishing Co., New York, 1955.